

RESOLUTION TEST CHART

AD-A188 488

OTIC FILE COPY

2

Resonance Energy Transfer Between Carbon Monoxide And Oxygen Molecules Using Dye
Laser Intracavity Absorption Spectroscopy

John W. Hrinishin, O-3
HQDA, MILPERCEN (DAPC-OFA-E)
200 Stovall Street
Alexandria, VA 22332

Final report - 21 October 1987

DTIC
ELECTE
DEC 15 1987
S D
D

Approved for public release; distribution unlimited

A thesis submitted to State University of New York at Buffalo, Buffalo NY, in
partial fulfillment of the requirements for the degree of Master of Arts in Physics.

87 12 8 135

REPORT DOCUMENTATION PAGE				Form Approved OMB No. 0704-0188	
1a REPORT SECURITY CLASSIFICATION			1b RESTRICTIVE MARKINGS		
2a SECURITY CLASSIFICATION AUTHORITY			3 DISTRIBUTION/AVAILABILITY OF REPORT		
2b DECLASSIFICATION/DOWNGRADING SCHEDULE					
4 PERFORMING ORGANIZATION REPORT NUMBER(S) Research on Energy Transfer between Carbon Mon- oxide and Oxygen Molecules using Dye Laser Intra- cavity Absorption Spectroscopy			5. MONITORING ORGANIZATION REPORT NUMBER(S) final report-October 1987 (87/10/21)		
6a NAME OF PERFORMING ORGANIZATION		6b OFFICE SYMBOL (if applicable)	7a NAME OF MONITORING ORGANIZATION		
6c ADDRESS (City, State, and ZIP Code)			7b ADDRESS (City, State, and ZIP Code)		
8a NAME OF FUNDING / SPONSORING ORGANIZATION		8b OFFICE SYMBOL (if applicable)	9. PROCUREMENT INSTRUMENT IDENTIFICATION NUMBER Student, HQDA, MILPERCEN (DAPC-GPA-E), 200 Stovall St., Alexandria, Virginia 22332		
8c ADDRESS (City, State, and ZIP Code)			10 SOURCE OF FUNDING NUMBERS		
			PROGRAM ELEMENT NO	PROJECT NO	TASK NO
			WORK UNIT ACCESSION NO.		
11 TITLE (Include Security Classification) HQDA, MILPERCEN, ATTN: DAPC-GPA-E, 200 Stovall Street, Alexandria, Virginia 22332					
12. PERSONAL AUTHOR(S) 21 October 1987					
13a. TYPE OF REPORT Thesis (final)		13b. TIME COVERED FROM 85/08/21 TO 87/10/21		14. DATE OF REPORT (Year, Month, Day)	15. PAGE COUNT 91
16. SUPPLEMENTARY NOTATION Approved for public release; distribution unlimited					
17 COSATI CODES			18. SUBJECT TERMS (Continue on reverse if necessary and identify by block number)		
FIELD	GROUP	SUB-GROUP	Thesis is unclassified. Submitted to the Faculty of the Grad- uate School of State University of New York at Buffalo in par- tial fulfillment of the requirements for the degree of Master		
19. ABSTRACT (Continue on reverse if necessary and identify by block number) of Arts. (SEE ATTACHED SHEETS)					
20. DISTRIBUTION/AVAILABILITY OF ABSTRACT <input checked="" type="checkbox"/> UNCLASSIFIED/UNLIMITED <input type="checkbox"/> SAME AS RPT <input type="checkbox"/> DTIC USERS			21. ABSTRACT SECURITY CLASSIFICATION		
22a NAME OF RESPONSIBLE INDIVIDUAL			22b TELEPHONE (Include Area Code)	22c OFFICE SYMBOL	

87 12 8 135

ABSTRACT

The dye laser intracavity absorption spectra of carbon monoxide and its mixtures with oxygen and helium in a plasma have been studied in the optical region between 5790 Å and 6080 Å. The purpose was to investigate possible resonant energy transfer between carbon monoxide and oxygen. A radio frequency discharge was used to excite the carbon monoxide gas to the upper vibrational levels of its ground electronic state from which optical excitation was performed by the dye laser to higher energy levels. The transition bands of the Fourth Positive System ($X^1\Sigma^+ - A^1\Pi$) were observed in the CO spectrum where the initial states were identified as $v=26$ to 46 of the ground electronic state. Anomalous effects in the line intensities in the CO spectrum taken at 1 Torr were observed when oxygen was added at partial pressures between 0.01 and 2 Torr. ←

As a follow-up to an earlier investigation, one region between 5913 Å and 5923 Å in the CO spectrum was measured for relative intensity changes as oxygen was added. Results generally indicated a slight increase for this region and for adjacent sections. Selected measurements varied but there was no anomalous change of this region in relation to the remaining spectrum. Poor mismatch in the vibrational level spacing ($\Delta E=650 \text{ cm}^{-1}$) between the upper vibrational levels for CO and those vibrational levels of the Rydberg $C^3\Pi_g$ state for oxygen provided a major argument against vibrational energy transfer. Using an apparatus configuration with less spectral resolution, the entire optical region 5790 Å and 6080 Å was examined for changes. Between 6000 Å and 6060 Å, the intensity in the lines in the CO spectrum was relatively high in comparison to other parts of the

spectrum. As oxygen was added, the intensity in the region was suppressed while changes in other parts increased or remained the same. Vibrational resonance energy transfer seems possible between $v=40 X^1\Sigma$ state of CO and $v=0 C^3\Pi_g$ states of O_2 ($\Delta E=150 \text{ cm}^{-1}$), although it cannot be confirmed since final states could not be observed.

(Item 10 Complete--Return to DD Form 1473)

Accession For	
NTIS CRA&I	<input checked="" type="checkbox"/>
DTIC TAB	<input type="checkbox"/>
Unannounced	<input type="checkbox"/>
Justification	<input type="checkbox"/>
By _____	
Date _____	
Approved _____	
Date _____	Approved _____
A-1	



RESONANCE ENERGY TRANSFER BETWEEN CARBON MONOXIDE
AND OXYGEN MOLECULES USING DYE LASER INTRACAVITY
ABSORPTION SPECTROSCOPY

by

John W. Hrinishin

A dissertation submitted to the Faculty of the
Graduate School of State University of New York
at Buffalo in partial fulfillment of the
requirements for the degree of

Master of Arts

October 1987

Dedicated to my beloved wife, Heike, and son, Michael

ABSTRACT

The dye laser intracavity absorption spectra of carbon monoxide and its mixtures with oxygen and helium in a plasma have been studied in the optical region between 5790 Å and 6080 Å. The purpose was to investigate possible resonant energy transfer between carbon monoxide and oxygen. A radio frequency discharge was used to excite the carbon monoxide gas to the upper vibrational levels of its ground electronic state from which optical excitation was performed by the dye laser to higher energy levels. The transition bands of the Fourth Positive System ($X^1\Sigma^+-A^1\Pi$) were observed in the CO spectrum where the initial states were identified as $v=26$ to 46 of the ground electronic state. Anomalous effects in the line intensities in the CO spectrum taken at 1 Torr were observed when oxygen was added at partial pressures between 0.01 and 2 Torr.

As a follow-up to an earlier investigation, one region between 5913 Å and 5923 Å in the CO spectrum was measured for relative intensity changes as oxygen was added. Results generally indicated a slight increase for this region and for adjacent sections. Selected measurements varied but there was no anomalous change of this region in relation to the remaining spectrum. Poor mismatch in the vibrational level spacing ($\Delta E=650 \text{ cm}^{-1}$) between the upper vibrational levels for CO and those vibrational levels of the Rydberg $C^3\Pi_g$ state for oxygen provided a major argument against vibrational energy transfer. Using an apparatus configuration with less spectral resolution, the entire optical region 5790 Å and 6080 Å was examined for changes. Between 6000 Å and 6060 Å, the intensity in the lines in the CO spectrum was relatively high in comparison to other parts of the

spectrum. As oxygen was added, the intensity in the region was suppressed while changes in other parts increased or remained the same. Vibrational resonance energy transfer seems possible between $v=40$ $X^1\Sigma$ state of CO and $v=0$ $C^3\Pi_g$ states of O_2 ($\Delta E=150\text{ cm}^{-1}$), although it cannot be confirmed since final states could not be observed.

TABLE OF CONTENTS

	Page
TITLE PAGE	i
DEDICATIONii
ABSTRACTiii
ACKNOWLEDGEMENTS	vii
LIST OF FIGURES AND TABLES.viii
 CHAPTER	
I INTRODUCTION	1
References	6
II THEORY	7
2.1 Perturbation	8
2.2 Selection Rules.	10
2.3 Intensity of Absorption Spectral Lines	15
2.4 Singlet-Triplet Transitions	15
2.5 Radiationless Transitions and the Relaxation Process	16
2.6 Carbon Monoxide (CO) and Oxygen (O ₂) Molecules .	19
References	24
III EXPERIMENTAL TECHNIQUES	25
3.1 Dye Laser and the Absorption Cell	25
3.2 Discharge Setup	27
3.3 Electro-Optic Tuner, Signal Processing and Data Accumulation	27
3.4 Procedures Followed to Study Collisional Effects on Carbon Monoxide	29
References	33
IV RESULTS AND ANALYSIS	34
4.1 General Remarks	35
4.2 Region A (5913-5923Å) of Carbon Monoxide Spectrum	36
4.3 Possible Resonance Energy Transfer v=40 X ¹ Σ of CO and v=0 C ³ Π _g of O ₂	46
References	59

V CONCLUSION	60
APPENDIX A: Plots of Intensity Ratio vs O_2 Pressure with Helium for Region A	A1
APPENDIX B: Plots of Intensity Ratio vs. O_2 Pressure Without Helium for Region A	B1
APPENDIX C: Plots of Intensity Ratio vs. O_2 Pressure For Spectral Region 6000-6060Å (Region E).	C1

ACKNOWLEDGEMENTS

Sincere gratitude is given for the many people who have provided me the necessary support to complete this study. The highest respect goes to my advisor, Dr. G. O. Brink, whose guidance from the time of selecting the subject to the completion of the report has been invaluable. His critical comments and suggestions were key to my understanding and development throughout the entire investigation. I am also grateful to my colleagues whose suggestions have helped towards collecting and analyzing the data. Special thanks is directed to David Sheets, a doctoral candidate in the Department, who provided support especially in the assistance of modifying computer software necessary to analyze the data. Former colleagues Dr. Kyong Kim and Dr. Ashoke Banerjee helped in the acquaintance with the instrumentation. I also recognize the United States Army, which without its financial support and confidence, my education leading to this thesis would not have been possible. Particular thanks is also given to Marlene Kowalski who typed the manuscript. Finally and most important, I acknowledge the clerical assistance of my wife Heike who typed the first version of this report. Her unending patience, confidence and moral support were instrumental towards the preparation of this thesis.

LIST OF FIGURES AND TABLES

<u>Figure</u>	<u>Title</u>	<u>Page</u>
2.1	CO Potential Energy Diagram	20
3.1	Diagram of the Experimental Setup	26
4.1	Salih's CO and Mixed Spectrum (Region A)	35
4.2	CO and Mixed He-CO-O ₂ Spectra (Region A)	37
4.3	CO and Mixed CO-O ₂ Spectra (Region A)	41
4.4	CO and Mixed CO-O ₂ Spectra at Various Partial Pressures of O ₂ (Region A)	42
4.5	CO and Mixed CO-O ₂ Spectra at Various Partial Pressures of O ₂ (Region A)	43
4.6	Co and Mixed CO-O ₂ Spectra Between 5890-6030Å	47
4.7	CO, O ₂ and Mixed CO-O ₂ Spectra Between 5770-6077Å	49
4.8	Mixed CO-O ₂ Spectrum and Summed Spectra of CO and O ₂	52
 <u>Table</u>		
2.1	Comparison of Energies between the band origins of the upper vibrational levels of ground state CO and vibrational levels of C ³ Π _g and d ¹ Π _g for O ₂	23

CHAPTER I

INTRODUCTION

Energy transfer mechanisms involving diatomic molecules and in particular, carbon monoxide, have been studied extensively in recent years. There have been various theoretical and experimental studies about molecular collisional energy transfer which include such mechanisms as vibration to vibration (V-V) transfer, vibration to electronic (V-E) transfer, vibration to translation (V-T) transfer and rotational energy transfer. These processes have been examined in part due to the interest in molecular laser performance and their importance in chemical mechanisms.

Many of the previous discussions on CO regarding collision and radiative processes have been mainly limited to the infrared or ultraviolet regions of the spectrum. In addition, mechanisms such as self-exchange V-V energy in CO have been analyzed primarily at the lower vibrational levels of the ground state. Studies by Rich¹ and Brechignac²⁻³ are exceptions to this whereby the pumping to higher vibrational states was done by optical pumping and gas discharge techniques, respectively. Salih⁴ performed extensive work in the visible region of the spectrum identifying the initial states as the higher vibrational levels of ground state CO for thirty vibrational bands to higher electronic states using a microwave discharge and dye laser intracavity absorption (ICA) spectroscopy. He also conducted a quantitative analysis on the effects of adding helium and oxygen to CO in this same region (5700-6175Å). Prior to this, the role of O₂ as a collision partner with CO was generally limited to discussions involving the operation of the molecular CO laser.

Salih reported changes in relative intensities of the ICA absorption lines at different regions of the visible CO spectrum when two gases, He and O₂, were added. These intensity differences were noted when the pure CO spectrum was compared to the mixed spectrum of 0.5 Torr CO, 0.1 Torr O₂ and 12 Torr He. Different regions of the spectrum were identified as either enhanced or suppressed as the result of the addition of these gases.

A reexamination of these reported intensity changes has been conducted in this study. Again, as Salih, the dye laser intracavity absorption technique was the method used to examine intensity changes. Greater sensitivity over single-pass measurements⁵ make this technique for observing absorption spectra more desirable. The absorber which is located in the cavity of the dye laser consists of the gas or mixture of gases to be analyzed. The gases are excited into a weak plasma by a radio frequency discharge which differs from the microwave discharge used by Salih. Analysis of the absorption signal can be made anywhere within the tunable region of the dye laser. Further analysis was made of those spectral regions of CO where Salih reported line intensity changes when O₂ and He were added.

This report specifically investigates two regions of the CO spectrum. The first region, Region A (5913-5923Å), is reexamined where line intensities were reported to be suppressed when O₂ and He gases are added. Analysis of this region was made under similar conditions to those established by Salih in his work. Region A was also studied when only O₂ is added to CO with the elimination of He from the mixture. This later procedure was taken as an attempt to directly examine the interaction of these two gases alone. The results of the spectral changes observed for

Region A did not coincide with those obtained by Salih. The second region, Region E (6000-6060Å) of the CO spectrum, was also examined using a lesser resolved spectrum. Suppression of line intensities were noted in this region with the addition of O₂ to CO. The spectral changes in Region E have led to the possibility of resonant energy transfer between CO and O₂.

Changes of intensity in the CO spectra with the addition of O₂ could be the result of near-resonant energy transfer between upper vibrational levels of ground state CO and vibrational levels of an excited electronic state of O₂. The population densities of these upper vibrational levels for CO can be related to the changes in intensity of their respective vibrational bands. Salih has largely identified these upper vibrational levels (v=26 to 46) as initial states for bands assigned to the Fourth Positive System (X¹Σ-A¹Π) of CO. Suppression of line intensities in Region E where the band region of v=40 has been identified suggests that the addition of oxygen might be quenching the population density of that state. From vibrational constants outlined in Herzberg and Huber⁶, vibrational level v=0 of the C³Π_g electronic state for O₂ matches in vibrational energy with v=40 of the CO X¹Σ ground electronic state with an energy difference of approximately 150 cm⁻¹. Since the energy defect is small, V-V and V-E resonant energy transfer from CO to O₂ is possible. However, the results from this study cannot fully support this particular energy transfer process. Observation of a transition with the C³Π_g (v=0) as the initial state for oxygen when CO is added to O₂ would provide additional information necessary to support

this claim. Unfortunately, the visible spectral region for O_2 does not provide the opportunity to observe the intensity of such a transition with this initial state.

Discussion about energy transfer processes of these upper vibrational levels for CO cannot be limited to one type of energy transfer process. Treanor et al⁷ claimed in their theoretical study that V-T energy transfer becomes more dominant at higher vibrational energy levels where it competes strongly with V-V energy transfer processes. Therefore, intensity changes at these upper vibrational levels for CO may be the result of V-T energy transfer with O_2 rather than resonance V-V or V-E energy transfer. This may be especially true at the $v=40$ level for CO as discussed above.

DeLeon and Rich¹ also claimed in their study of CO that the V-E energy transfer coupling at vibrational levels of 40 and greater of the ground state became strong with the excited electronic state, $A^1\Pi$, for CO. This effect, if true, could ultimately influence energy transfer between CO and O_2 at these higher vibrational levels.

Another factor regarding energy transfer mechanisms involves the weak plasma conditions under which both gases are examined. There are numerous competing mechanisms in a plasma which may affect the energy transfer process between CO and O_2 . Newly created by-products as a result of induced reactions in the plasma could affect the population density of observed states in the spectra for CO and O_2 . As a result, observed intensity changes may be merely the effects of these outside influences when oxygen is added to CO and not resonant energy transfer between the two molecular systems.

One other possible influence on intensity changes observed in the CO spectrum is the effect the addition of oxygen has on lowering the average electron energy in the plasma⁸ where excitation of CO is favored. The change in partial pressure of the added O₂ will in turn change the average electron energy, the source that ultimately populates the higher vibrational levels of CO.

This study will report on the line intensity changes of the CO spectrum with the addition of O₂ and He and on possible evidence of resonant energy transfer between CO and O₂. Those factors, as mentioned above, are important towards determining as to whether such an energy transfer process occurs. Although conclusive evidence is lacking to definitely state that resonant energy transfer between CO and O₂ does occur, there are line intensity changes in the CO spectrum which indicate the possibility.

References

1. J.E. Rich, R.L. DeLeon, "Vibrational Energy Exchange Rates in Carbon Monoxide", Arvin/Calspan Advanced Tech. Ctr., Buffalo Contract No. DASG60-84-C-0047 for USAMDATC.
2. P. Brechignac, J.P. Martin, G. Taieb, "Small-Signal Gain Measurements and Vibrational Distribution in CO", IEEE Journal of Quant. Mech., Vol. QE-10, 10, 797 (1974).
3. P. Brechignac, "Near-Resonant V-V Transfer Rates for High Lying Vibrational States of CO", Chemical Physics, 34, 119 (1978).
4. A. Salih, "Dye Laser Intracavity Absorption Spectrum of Carbon Monoxide" Ph.D. Thesis, SUNY at Buffalo, 1986,
5. P. Kunmar, G. O. Brink, S. Spence, H.S. Lakkaraju, "Line Shape Studies in CW Dye Laser Intracavity Absorption", Optics Communications, Vol. 32, 1, 129 (1980).
6. K. P. Huber, G. Herzberg, "Constants of Diatomic Molecules", Van Nostrand Company, New York, 1979.
7. C. E. Treanor, J. W. Rich, R. G. Rehm, "Vibrational Relaxation of Anharmonic Oscillators with Exchange-Dominated Collisions", Journal of Chem. Physics, Vol. 48, 4, 1798 (1962).
8. E. M. Osgood, W. C. Eppers, E. R. Nichols, "An Investigation of the High-Power CO Laser", IEEE Journal of Quant. Mech., Vol. QE-6, 3, 145 (1970).

CHAPTER II

THEORY

The complexity of the electronic spectra for a mixed gas is immense due to the numerous lines caused by various overlapping and perturbation effects. Even the spectra for only one diatomic molecule such as CO proves to be a formidable task to analyze.

The reason for this complexity arises in part from the stimulation of simultaneous vibrational and rotational transitions when an electronic transition takes place. As the electron distribution is changed by such an electronic transition, the nuclei must adjust to the new force field by moving in vibration. This change of vibration, in turn, affects the rotational state of the molecule. To further complicate the issue, each molecule possesses its own sources of angular momentum. The types of coupling of these angular momenta as defined by Hund are different for each electronic state. Herzberg¹ describes Hund's five modes of coupling in detail. These modes of coupling and variations thereof as influenced by the different rotational and electronic motions of the molecule determine the quantum numbers. The quantum numbers define the rotational levels and their energies in each electronic state. This provides information on what symmetry properties the corresponding eigenfunction possess. By knowing these symmetry properties of an eigenfunction and the forms of outside interactions of perturbations on the system, we can estimate the new transition probabilities and changes in energy of the system. Therefore, by applying a radiation field or by adding a different molecular gas to a single or multiple gas system, a host of new interactions occur changing transition probabilities and intensities of a spectrum.

2.1. Perturbations

A system can be defined by choosing which interactions to include in the Hamiltonian and employing the Schroedinger equation

$$H_0 \Psi_j = E_j \Psi_j \quad (j = 1, 2, 3, \dots) \quad (2.1)$$

for the unperturbed case. In terms of the unperturbed eigenvalues and eigenfunctions, using the perturbation theory, an "adjusted" set of new eigenvalues and eigenfunctions can be developed to account for the added "environmental" perturbation, H_p . The Schroedinger equation is changed accordingly to

$$(H_0 + H_p) \Psi_j = E_j \Psi_j \quad (j = 1, 2, 3, \dots) \quad (2.2)$$

The new eigenvalues for a non-degenerate case up to the second approximation are (see Pauling and Wilson² for example)

$$E_j = E_{0j} + H_{Pjj} + \sum_{\ell \neq j} \frac{|H_{Pj\ell}|^2}{E_{0j} - E_{0\ell}} \quad (2.3)$$

where

$$H_{Pj\ell} = \int \Psi_j^* H_p \Psi_\ell d\tau \quad (2.4)$$

in which $H_{Pj\ell}$ is the perturbation Hamiltonian of the "matrix element $j\ell$ ". A quick examination of equation 2.3 will show that the shift of a given level depends inversely on its separation from the other energy levels. The smaller the separation between the two levels the larger are their shifts on account of the perturbation Hamiltonian. A repulsive effect takes place on the two energy levels where the upper level is moved up and the lower one is moved down. The wavefunction corrected to first order in the perturbation is described as

$$\psi_j \cong \psi_{0j} + \sum_{\ell} \frac{H_{\ell j}}{E_{0j} - E_{0\ell}} \psi_{0\ell} \quad (2.5)$$

In addition to the energy level separation, the magnitude of the matrix element (see equation 2.4) of the perturbation Hamiltonian contributes directly to the magnitude of the perturbation itself. In other words, the symmetry properties of the eigenfunctions for each state, as described earlier, are responsible for the magnitude of the perturbation.

Perturbations such as molecular collisions and radiative fields impose these changes on energy states over the period of the perturbation. These time-dependent perturbations affect transition probabilities between states, the rates of transitions and the intensities of spectral lines. An important relation to determine the transition probability between two states is the Born Approximation.

$$P_{j\ell} = \frac{1}{\hbar^2} \left| \int_{t_0}^{\infty} H_{p\ell j}(t) \exp(i\omega_{\ell j}t) dt \right|^2 \quad (2.6)$$

This relation can be derived³ starting with Schroedinger's Equation where $P_{j\ell}$ represents the probability of a transition from state j to state ℓ . From time-dependent perturbation theory, the approximated interaction (i.e. dipole-dipole, etc.) is determined and incorporated into the above expression for the transition probability. As a result, there are two features for molecular energy transfer which can be seen from the Born Approximation. First, the perturbing Hamiltonian must couple states j and ℓ before transitions may be induced between them. Secondly, the concept of resonance in molecular energy transfer is strongly supported since the probability depends on the Fourier components of the time dependent perturbation, $H_p(t)$, at the frequency $\omega_{\ell j}$. For example, energy transfer is

most efficient when the reciprocal of the interaction time multiplied by \hbar is equal to the energy defect between the initial and final states⁴.

$$\frac{\hbar}{t} = E_{\ell} - E_j \quad (t \Rightarrow \text{interaction time}) \quad (2.7)$$

where $E_{\ell} - E_j = \hbar (\omega_{\ell j} - \omega) = E_{\ell}$ (excited molecule, no photon) - E_j (ground state, photon $\hbar\omega$)

The time-dependence of the probability of being found in state ℓ depends on the frequency offset $\omega_{\ell j} - \omega$. When the frequency offset is zero, the perturbation and the system are in resonance, and the transition probability increases most sharply.

Spectral intensities are proportional to transition rates because they depend on the rate of change at which energy is absorbed from an electromagnetic field or pumped into it. The transition rate, $W_{j\ell}$, is defined to be the time rate of change of the transition probability from state j to state ℓ ¹⁴.

$$W_{j\ell} = \frac{d}{dt} P_{j\ell} \quad (2.8)$$

This expression is key towards defining the Beer-Lambert Law which is discussed in section 2.3.

2.2. Selection Rules

The probability of a transition for a system of molecules under the influence of radiation or any other perturbation is determined by the eigenfunctions of the upper and lower states. Therefore, the prescribed symmetry properties of the eigenfunctions as mentioned earlier are important as to whether a given transition may occur (allowed) or not (forbidden). Time dependent perturbation theory shows that the transition rate depends on

the square of the matrix element, $H_{P_{j\ell}}$ of the perturbation. The electric dipole interaction as expressed by H_P is the strongest interaction. For the first approximation:

$$H_P = - \vec{u} \cdot \vec{\epsilon} \quad (2.9)$$

where \vec{u} is the electric dipole moment operator for the molecular system and $\vec{\epsilon}$ is the oscillating electric field. (In most cases, the radius of the molecule is considered much smaller than the wavelength of the $\vec{\epsilon}$ field allowing $\vec{\epsilon}$ to be constant.) The matrix element, $H_{P_{j\ell}}$ has been given as equation 2.4 using eigenfunctions Ψ_j and Ψ_ℓ . If $H_{P_{j\ell}}$ has a non-zero element, the transition is then said to be allowed. This formulation establishes certain rules known as the selection rules. The symmetry of the matrix element or transition moment, $H_{P_{j\ell}}$ establishes the details for these rules. For an electric dipole interaction, the selection rules for a diatomic molecule can be summarized as follows:

$$\begin{aligned} g \leftrightarrow u \quad g \leftrightarrow g \quad u \leftrightarrow u \quad (\text{homonuclear molecule}) \\ \Delta J = 0, \pm 1 \quad \text{but } J = 0 \leftrightarrow J = 0 \text{ and for } \Omega = 0 \rightarrow \Omega = 0, \Delta J \neq 0 \\ \Delta \Lambda = 0, \pm 1 \quad \Delta \Omega = 0, \pm 1 \\ \Delta S = 0, \quad \Delta \Sigma = 0 \quad (\text{for weak spin-orbit coupling}) \\ + \leftrightarrow +, \quad - \leftrightarrow -, \quad + \leftrightarrow - \end{aligned} \quad (2.10)$$

J = total angular momentum, Λ = component of total electronic orbital momentum along the internuclear axis

Ω = total electronic angular momentum along internuclear axis ($\Omega = \Lambda + \Sigma$)

These are the generalized selection rules for electronic transitions. In Herzberg¹, the different Hund's cases define these rules even further.

The selection rules for interactions involving molecular collisions have been generally categorized under the perturbations considered by Kronig⁵. Different energy transfer mechanisms resulting from collisions can host a variety of interactions with different strengths. Depending on which interactions are considered as a result of a molecular collision, the selection rules can vary accordingly. However, for perturbations which include collisional energy transfer processes, Kronig's selection rules are generally used based on the quantum number and symmetry properties of the two states involved. These rules can be summarized as follows:

- 1 - sym \leftrightarrow antisym
- 2 - $\Delta J = 0$
- 3 - $\Delta \Lambda = 0, \pm 1$ $\Delta \Omega = 0, \pm 1$
- 4 - $\Delta S = 0$
- 5 - + \leftrightarrow +, - \leftrightarrow -, + \leftrightarrow - (2.11)

Rules one, two, and five are rigorous. Rule one prohibits the intercombination of symmetric and antisymmetric states and is especially important for homonuclear molecules such as O_2^{16} where rotational states with $\Lambda = 0$ will alternate in symmetry.

Selection rules for vibrational transitions without electronic excitation are again derived from the transition moment

$$\int \psi_e^* \psi_v^* \vec{u} \psi_e \psi_v d\tau \quad (\text{assuming } \epsilon \text{ constant})$$

$$\vec{u} = \sum_i e_i \vec{v}_i \Rightarrow \text{dipole moment displacement} \quad (2.12)$$

whereby the expression after the electronic wavefunctions are factored out becomes

$$\int \psi_{v'}^* \vec{u} \psi_v d\tau_v \quad (2.13)$$

The Born-Oppenheimer approximation allows the electronic and vibrational wavefunctions to be separated essentially on the argument that the massive nuclei move slower than the electrons and may be considered at rest. After expanding the transition matrix to the first approximation, the second term of the expansion is non-zero so long as the dipole moment depends on the displacement of the two nuclei. The specific selection rule is established as $v=v\pm 1$. There is a possibility that the dipole moment displacement is significant at the higher order terms of the expansion resulting in those derivatives being non-zero. In such cases, Δv may equal 2,3,4 etc. at which these transitions occur as weak overtones.

During electronic excitation, equation 2.6 is evaluated at constant internuclear distance whereby a vertical transition occurs between the two electronic states. This is known as the Franck-Condon principle. The overall transition dipole moment in this case can be expressed as

$$\vec{u}_{e'e} \int \psi_{v'}^* (\vec{R}) \psi_v (\vec{R}) d\tau_v = \vec{u}_{ee'} S_{v'v} \quad (2.14)$$

The term $\vec{u}_{ee'}$, represents a constant based on the approximation that the integral for the transition moment of the electronic transition is constant when the nuclear coordinate, \vec{R} , has some fixed value. $S_{v'v}$, represents the overlap integral of the two vibrational states. Therefore, the transition moment is the largest when the vibrational wavefunction of the vibrational states of the upper electronic level has the greatest overlap with the wavefunction of the initial vibrational state of the lower electronic level.

In order to identify the upper vibrational level where the transition will end, the upper level that most resembles the initial state with the bell-shaped gaussian function would have to be considered. Such transitions would indicate relative strong intensities and would be proportional to $S_{v'v}^2$. In this case, the selection rules allow vibrational transitions with $\Delta v = 0, \pm 1, \pm 2, \dots$

Since the resolution of the spectrum was decreased in part of the study for the purpose of obtaining a wider view of the spectrum, the individual rotational transition lines were not observed (further explanation of this is provided in Chapter 3). However, the selection rules for rotational transitions are set out in equation 2.10. The $\Delta J = 0, \pm 1$ transitions give rise to the P-, Q-, and R- branches in the spectrum. Vibration-rotation spectra will differ in the appearance of each branch in regard to line spacing and intensity. One reason for this is that the rotational constants for each electronic state differ considerably due to the different bond lengths for each state. The presence of Λ -doubling effects and complications from perturbations between one state and another are other reasons for the difference in appearances of these branches. Examples of such perturbations includes the change in energy of each state when wavefunctions of the same symmetry approach each other. In this case, the non-crossing rule must be obeyed where potential curves of two electronic states of the same species cannot cross each other. The process of predissociation also causes a mixing of energy levels whereby an upper electronic state is perturbed by a dissociative state. For a molecule in the excited state where the energy level crosses in terms with the dissociative state, the molecule may dissociate or separate. This, in turn, reduces the lifetime of the molecules in this region which produces

increasing atomic number, the limitation of such intercombination becomes less. Such bands do occur when in the molecule there is present a heavy atom, having a large spin orbit coupling constant. Yardley³ provides a discussion showing how the spin-orbit coupling Hamiltonian can act as a perturbation to mix singlets and triplets. Carbon monoxide, CO, has been shown to have singlet-triplet intercombinations despite it being a relative light molecule. The $^3\Pi-^1\Sigma$ transition (Cameron bands) for CO have been observed¹.

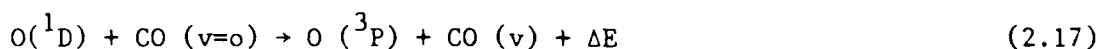
Occurance of the singlet-triplet intercombination can be the result of perturbations between states of fairly large separation and of the same Ω , total electronic orbital axial momentum. If a $^1\Sigma$ state is perturbed by $^3\Pi_0$ state for example, the former may combine with a $^3\Sigma$. The mixing of eigenfunctions of the $^1\Sigma$ and $^3\Pi_0$ states will extend properties to each other where the $^1\Sigma$ will weakly combine with the $^3\Sigma$ state. Such intercombinations do occur as the result of intermolecular collisions since transitions involving change of multiplicity are not strictly forbidden.

2.5. Radiationless Transitions and the Relaxation Process

In this experiment, an RF discharge was used to non-selectively excite the CO molecule to higher vibrational levels of its ground electronic state. Absorption of radiation from the dye laser further excited CO molecules to higher excited states as discussed in the introduction. It is known that molecules once excited will return to their ground state. A possible mode of return is by decay involving radiationless transitions. If the excited molecule is subjected to frequent collisions, then the colliding species may

act as an acceptor for the excess energy. Electronic energy of an excited atom, for instance, can be transferred through collisions into the vibrational modes of molecules of the system. This is known as electronic to vibrational (E-V) energy transfer. This energy can be dispersed even further into the system by means of collisions whereby the vibrational energy is transferred into the rotational and translational degrees of freedom of the system. The method by which this excitation energy is degraded into thermal motion is referred to as a relaxation process. The direction of this process is determined by the direction of increasing entropy.

Electronic-to-vibrational (E-V) energy transfer studies have involved systems where transfer of energy occurs between an electronically excited atom to a molecule, or by the reverse process from a vibrationally excited molecule to an unexcited atom. An example of this process could be one which can be found to occur between CO and O₂. Slanger and Black⁵ reported on the E-V process



In this case, through photolysis, O₂ molecules were excited into oxygen (¹D) atoms with light at 1470Å. The oxygen atoms were energetic enough to vibrationally excite CO to v=7. Under the Resonant Theory developed by Shamu et.al.⁶, this electronic relaxation process is due to some collisional perturbation where long-range interactions such as dipole-dipole, quadrupole-dipole or quadrupole-quadrupole are involved. By applying the Born Approximation (equation 2.6) these interactions can be used to ultimately provide some understanding of the energy transfer process. However, in some cases, the first approximation is not

satisfactory since some of these interactions may shift the corresponding energy levels of the two colliding particles. Another approach which Yardley³ describes is called the "curve crossing" mechanism that pursues the effects of the perturbation on the potential curves where the variation in energy of the initial and final states is examined. Kaufman⁷ provides the theoretical background for this more sophisticated approach.

Another type of relaxation process is the V-T energy-transfer mechanism. CO is an excellent example of a diatomic gas where numerous studies have been made on its V-T relaxation with itself and other gases. The relative large vibrational frequency region of CO allows the relaxation process to be closely examined when added to quenching gases such as helium. Helium leaves no V-V energy transfer avenue available for CO but it does allow itself to be translationally excited while vibrationally relaxing CO. At room temperature He is approximately 20 times more effective in quenching CO than CO itself due to its much smaller mass. Helium's ability to increase thermal conductivity in CO gas mixtures appears to be its prime role in molecular CO lasers. There have been classical and semi-classical systems established to describe theoretically the V-T energy transfer for simple colinear collisions between a diatomic molecule and an atom. Such studies⁷ have determined the probability of this energy transfer using models of harmonic oscillators changing from initial to final state as a result of molecular collisions.

Rotational energy transfer will only be briefly mentioned but it has some major differences from vibrational and electronic energy transfer mechanisms. Most of the differences arise from the fact that the rotational energy levels are spaced closer than kT . In addition to the close spacing,

the high level of degeneracy of the rotational levels, without any outside perturbations, make it difficult to determine which quantum process is involved. There could be numerous avenues for the energy to transfer by. Again, the Born Approximation is used to analyze the interaction potential and to develop general selection rules for rotational energy transfer. However, different approaches using the above guidelines have met only limited success.

One other energy transfer mechanism which is addressed extensively in the discussion portion of this report, is the vibration-to-vibration (V-V) energy process. Treatment of this process, theoretically, is very similar to the V-T process except a linear encounter of two diatomic molecules is assumed with each being considered a harmonic oscillator. Rapp and Kassel⁹ provide a detail analysis of such a model. The Born Approximation is again used to include the types of interaction potentials to determine the transition probability for such a collision. Situations such as near or non-resonant V-V relaxation caused by long-range interactions are discussed in length.

2.6. Carbon Monoxide (CO) and Oxygen (O₂) Molecules

Carbon Monoxide is a heteronuclear diatomic molecule whose bond distance between atoms in the ground state is 1.1 Å. CO possesses a permanent dipole moment and has a ionization potential of 14.009 eV. The potential energy diagram for CO is shown as Fig. (2.1). The ground electronic state is the $X^1\Sigma^+$ state. The potential energy curve for this state forms a deep well and overlaps some of the excited states. The first excited state is the $a^3\Pi$ state, a metastable state, since transition from

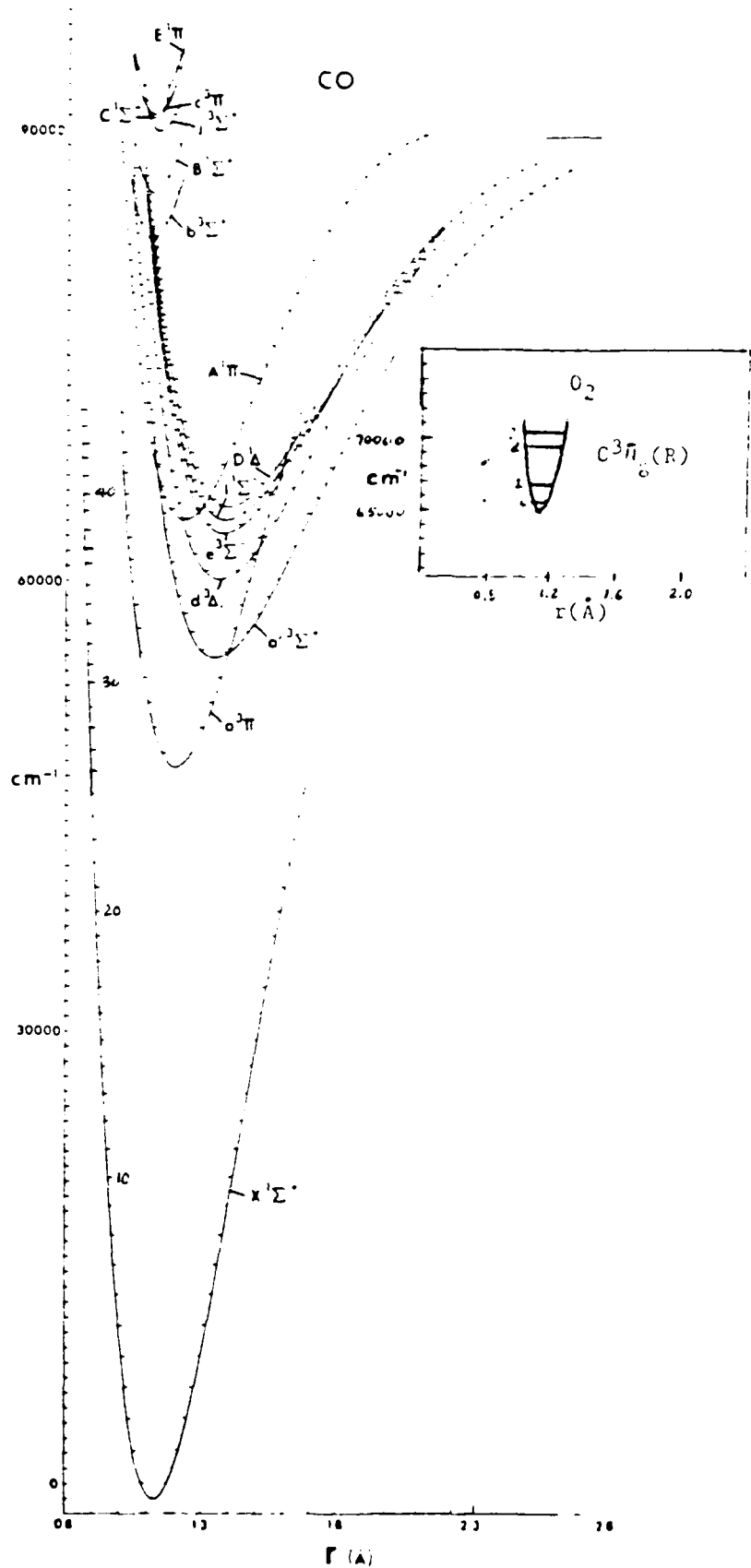


Fig. 2.1 CO Potential Energy Diagram. Highlighted is the Potential Energy Curve of the $C^3\Pi_g$ electronic state for O_2 . Vibrational Energies for this state₁ can be compared to those energies of the upper vibrational levels in the $X^1\Sigma^+$ state for CO.

this state to the ground state are forbidden. The first excited singlet state is the $A^1\Pi$ state where transitions from the ground $X^1\Sigma^+$ state are allowed. The transition band between these two states is designated as the Fourth Positive System. However, under a normal Boltzmann population distribution, the highest populated states are found at the lowest vibrational and rotational levels of the ground electronic state. Radiation in the ultraviolet region of approximately 64000 cm^{-1} is needed to excite these molecules to the $A^1\Pi$ state. This requirement can be circumvented by exciting the CO molecules to higher vibrational levels of the ground state and then allowing the absorption of a visible light quantum to provide the necessary energy to excite those states to higher electronic state. One method to excite CO to those higher vibrational levels is by gas discharge. Brechignac et al⁸ have studied the upper vibrational levels of CO by using an electrical discharge. The disadvantage of this method is that this means of excitement is non-selective whereby all states are excited by the electron bombardment. As a result, numerous different transitions occur which can complicate the spectrum tremendously. Our interest is in higher populated vibrational states where transitions to the $A^1\Pi$ state and other excited states can be observed.

Oxygen, in contrast to CO, is a homonuclear molecule whose bond distance between atoms in the ground state is 1.2074 \AA . The ionization potential for O_2 is 12.1 eV . The two unpaired electrons of the outer orbital in the ground state give rise to paramagnetic properties for this molecule. The ground state for O_2 is the $^3\Sigma_g^-$ state. The next two higher electronic states are the $^1\Delta_g$ and the $^1\Sigma_g^+$ states, each with singlet

multiplicity. Analysis of the so-called "atmospheric bands" in the visible region as investigated by Herzberg¹ revealed they originated in the ${}^3\Sigma_g^- \rightarrow {}^1\Sigma_g^+$ transition and placed this 13065 cm^{-1} above ground state. The existence of the ${}^3\Sigma_g^- \rightarrow {}^1\Delta_g^+$ band was also shown to exist in the near IR spectrum. Since both of these transitions are forbidden, intensities were found to be extremely weak.

Herzberg and Huber¹¹ list two excited electronic states in the region of interest coinciding with the higher vibrational levels for CO. They are designated as the $C^3\Pi_g$ and $d^1\Pi_g$ states with the electronic energies of 65530 cm^{-1} and 69180 cm^{-1} , respectively. Both of these states overlap high vibrational levels of the ground state of CO. Table 2-1 depicts the vibrational energy levels¹²⁻¹³ of both electronic states for O_2 with those upper vibrational levels of the ground state for CO.

TABLE 2-1

COMPARISON OF ENERGIES* BETWEEN THE BAND ORIGINS OF THE UPPER VIBRATIONAL
LEVELS OF GROUND STATE CO AND VIBRATIONAL LEVELS OF
 $C^3\Pi_g$ AND $d^1\Pi_g$ FOR O_2

CO ($X^1\Sigma$)		O_2 ($C^3\Pi_g$)		O_2 ($d^1\Pi_g$)	
$E(\text{cm}^{-1})$	v	v	$E(\text{cm}^{-1})$	v	$E(\text{cm}^{-1})$
				—2	72953
71282	45—	—3	71239		
70238	44—	—2	69460	—1	71186
69170	43—			—0	69323
68077	42—	—1	67496		
66960	41—				
65820	40—	—0	65665		
64655	39—				
63466	38—				
62252	37—				
61015	36—				

* Zero energy has been established at the $v=0$ vibrational level
of the ground electronic state for both molecular systems

References

1. G. Herzberg, "Molecular Spectra and Molecular Structure", Volume 1, 2nd Edition, Van Nostrand Reinhold Company, N. Y., 1950.
2. L. Pauling, E.B. Wilson, "Introduction to Quantum Mechanics", McGraw-Hill Book Company, Inc., New York, 1935.
3. J. J. Yardley, "Introduction to Molecular Energy Transfer", Academic Press, New York, 1980.
4. N. Mataga, T. Kubota, "Molecular Interactions and Electronic Spectra", Marcel Dekker Inc., New York, p. 9 1970.
5. R. De L. Kronig, Z. Physik 62, 300 (1930).
6. R. D. Sharma, C.A. Brau, "Energy Transfers in Near-Resonant Molecular Collisions due to Long Range Forces with Application to Transfer of Vibration Energy from ν_3 Mode of CO_2 to Ne", J. Chem. Physics, 50 924 (1969).
7. J. J. Kaufman, Advanced Chemical Physics 28, 113 (1975).
8. D. Rapp, "Quantum Mechanics", Chapter 24, Holt, New York, 1971.
9. D. Rapp, J. Kassel, Chem. Rev. 69, 61 (1969).
10. P. Brechignac, "Near-Resonant V-V Transfer Rates for High Lying Vibrational States of CO", Chemical Physics, 34, 119 (1974).
11. G. Herzberg, K.P. Huber, "Constants of Diatomic Molecules", Van Nostrand Company, New York, 1979.
12. R. H. Huebner, R. J. Celott, S. R. Mielczanek, C. E. Kuyatt, "Apparent Oscillator Strengths for Molecular Oxygen Derived from Electron Energy loss Measurements", J. Chem. Phys. Vol. 63, 1, 241 (1975).
13. S. Trajmar, D. C. Cartwright, R. I. Hall, "Electron Impact Excitation of the Rydberg States in O_2 in the 7-10 eV/energy-loss region", J. Chem. Phys., Vol. 65, 12, 5275 (1976).
14. A. Bohm, "Quantum Mechanics", Springer-Verlag New York Inc., New York p. 308, 1979.

Chapter III

Experimental Techniques

Fig. 3.1. depicts the experimental setup used in this study. The rhodamine 6G dye laser which is pumped by an argon ion laser has been described previously¹⁻². The absorption cell is located along the long leg of the cavity where the laser light is absorbed by the gas or gases to be analyzed. Wavelength sweeping of the dye laser is accomplished by an electro-optic tuner. A radio-frequency discharge provided power to the entrapped gas by means of two copper electrodes placed on a cylindrical glass tube of the vacuum system. Reflection from one of the brewster windows on the absorption cell provided an output signal to the spectrograph. The dispersed light was detected by the vidicon which sent the data directly to the on-line computer where the information was processed and stored.

Brief description of the equipment and details of the procedure is provided in this chapter.

3.1. Dye Laser and the Absorption Cell

As shown in figure 3.1., the dye laser consists of a folded, three mirror resonator with free flowing jet stream of dye-solution set at Brewster angle. A Spectra Physics (5 Watt, Model 165) argon ion laser is the pump laser which is focused to a small spot in the dye stream using a convex lens. The dye solution is composed of the dye, rhodamine 6G, dissolved in ethylene glycol. The pump laser is centered on the dye stream at the point of minimum mode diameter where the emission intensity has the maximum value. The angle between the long and short legs of the cavity, where the vertex is the folding mirror, compensates for the astigmatic aberration introduced by the thickness of the dye stream. The long leg of

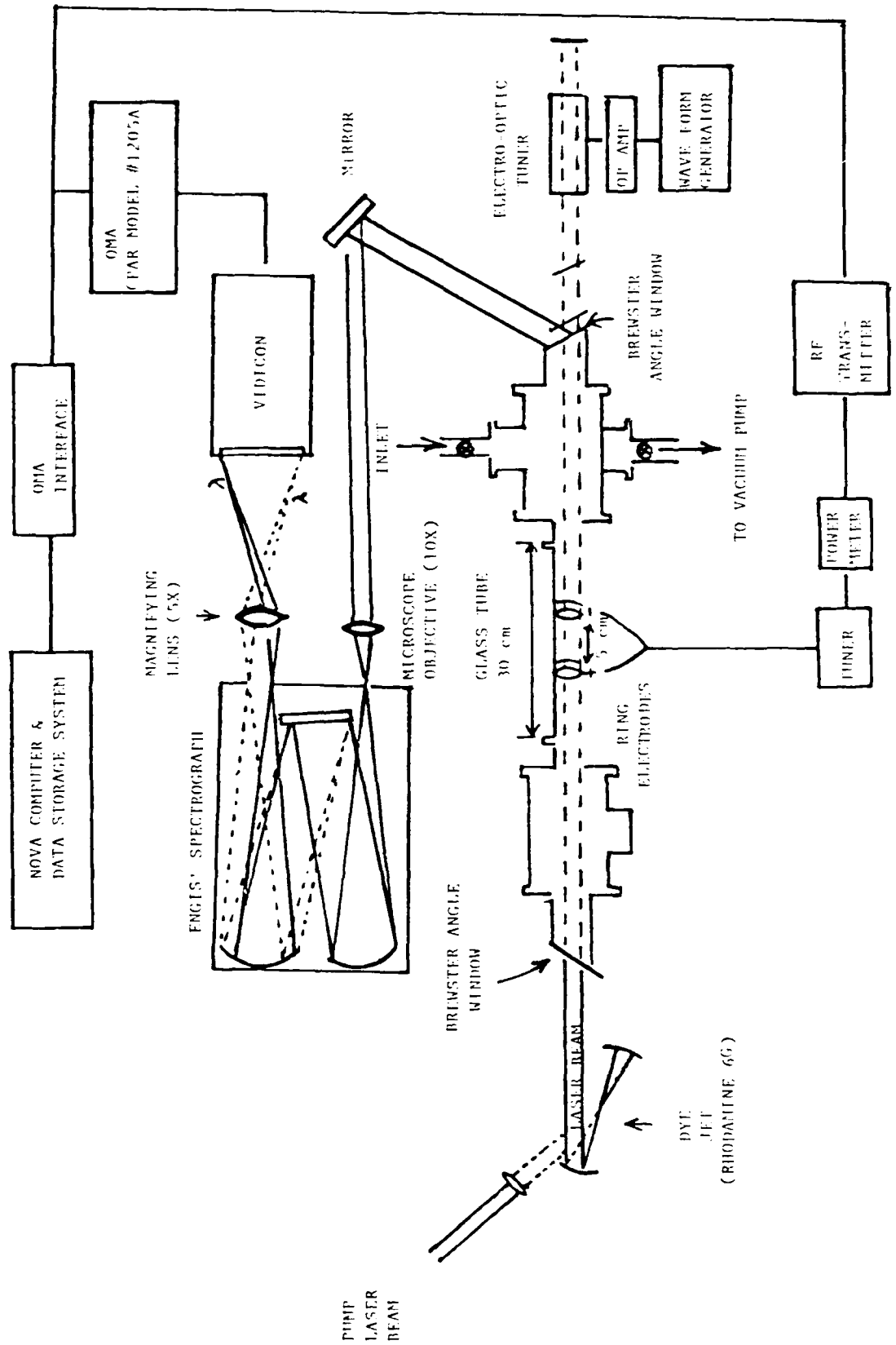


FIG. (3.1) DIAGRAM OF THE EXPERIMENTAL SETUP WITH RF DISCHARGE SYSTEM

the cavity provides space where the vacuum assembly with brewster windows is mounted to form the absorption cell. This is also the location where the optical tuner is placed. For further details regarding dye laser cavities see Kogelnik³ and Holt⁴.

The absorption cell is optically aligned along the long leg of the dye laser. Inlet and outlet valves controlled the flow of gases in and out of the system. Data was collected under static conditions. A vacuum pump evacuated gases as desired to pressure as low as 30 millitorr, however, lower pressures could have been achieved by means of a diffusion pump connected in line with the system. The pressure inside the vacuum chamber was measured by a 10 Torr baratron.

3.2. Discharge Setup

Excitation of the gas is done by two copper electrodes powered by a radio transmitter wrapped around the center region of a glass tube cavity of the absorption system. A radio frequency of 3.65 MHz passes through a power meter and a tuner before reaching the electrodes. A forward power setting of 40-50 Watts and reflected power of 5-7 Watts was maintained throughout the experiment. The pyrex tubing which houses the gases is approximately 30 cm in length and about 1.2 cm in diameter. At pressures of 1 Torr and less for CO, the glow from the discharges extends beyond the full length of the tubing. The discharge excites the gas molecules to an intermediate excited state by electron bombardment from which optical excitation is performed by the dye laser to higher energy levels.

3.3. Electro-Optic Tuner, Signal Processing and Data Accumulation

The optical tuner provides wavelength control of the dye laser. The device is aligned along the axis of the long leg of the laser cavity and its tuning crystal provides control of the laser output wavelength in response to an applied voltage. It is driven by a Burleigh high voltage amplifier which amplifies a triangular waveform from a wavetek signal generator. A sweep rate of 200 Hz was used throughout the experiment as the optimum setting to obtain the ICA spectrum.

Reflection of the laser light from one of the brewster windows provides the output signal as depicted in figure 3.1. The signal was sent to a Hingler-Engis Model (600) monochromator using a 1200 lines/mm. grating in first order. For the first part of the experiment where higher spectral resolution was desired, a magnifying lens (5x) at the output slit of the monochromator was utilized. The lens dispersed the image signal resulting in a resolution ($\Delta\lambda$) of about 0.037 Å. The signal was focused onto an array of 500 detector elements in the vidicon. Because the width of each detector is only 0.001 inch, there is a "cross talk" effect⁵ between adjacent elements which lowers the resolution to about 0.074 Å. Under this arrangement, and 18 Å region of spectrum was scanned and processed.

Our interest in observing relative changes of intensity over a broader region of the spectrum led us to remove the magnifying lens between the output slit of the monochromator and the vidicon. The effect of this change concentrated the signal across the 500 detectors which expanded the spectral region to 187 Å and lowered the resolution to about 0.75 Å. Despite the ability to achieve this "187 Å view" of the spectrum, the maximum voltage setting on the high voltage amplifier limited the range of sweeping by the tuner to 140 Å. However, this set-up change provided a wide enough region of spectrum for our purposes to make the decrease in resolution acceptable.

The linear array of detectors in the vidicon are storage devices and each is read one at a time by a scanning electron beam. After the signal is amplified, dark current compensated, and digitized, the signal is sent to a NOVA 3 mini-computer through an interface built by Dr. S. Heider.

3.4. Procedures followed to study Collisional Effects on Carbon Monoxide

3.4.1. General

Salih⁶ reported on 5 regions of the CO spectrum where relative intensities of the absorption lines changed when helium and oxygen gases were added. One region, designated as Region A, was chosen to be studied in detail. Region A (5923-5913 Å) was reported to have a very significant, relative decrease in line intensity when the gases were added. This region also happens to be located in the center and optimum region of the dye gain curve where minimum laser threshold is least important as compared to the spectrum locations of the other regions. Therefore, CO spectrum Region A was selected for an extended study over varied gas pressures of CO, O₂ and He.

Results of this analysis using the lens arrangement which provides for higher resolution but a narrower 18 Å view of the spectrum shifted our interest towards reexamining the entire CO spectrum in the less resolved configuration. With the magnifying lens (5x) removed from the setup, the CO spectrum over a 140 Å wide region was analyzed. Despite lower resolution, this approach allowed for a direct examination of intensity changes across a larger portion of the spectrum which included most of 4 regions addressed in Salih's report. It was at this resolution which Region E (6000 - 6060 Å) was examined. Threshold of the dye laser and the pump power of the argon laser

were the factors limiting the extent to which the two extreme ends of the spectrum could be observed.

3.4.2. Procedures taken to Analyze Intensity Changes in Region A (5913-5923 Å)

The entire experiment was conducted for gases in the static, non-flow condition with total gas pressures ranging between 0.01 to 10 Torr. Spectra of carbon monoxide, oxygen and helium were taken separately in Region A over varied pressures within the above limits. Mixed Spectra of CO over varied partial pressures of O₂ and He followed. Spectra of gas mixtures with a pressure ratio of 95:4:1 for He, CO and O₂, respectively, were obtained to match Salih's ratio in his flow experiment. Spectra in this region were also taken of CO at 1 Torr with just the addition of O₂ between 0.01 and 2 Torr without helium. All this work was performed using the greater resolution configuration, ($\Delta\lambda = 0.37\text{\AA}$),

Throughout the experiment, the pump argon laser power was kept between 0.9 and 1.3 watts with the dye laser optically aligned for thresholds between 0.6 to 0.7 watts. Leak detector tests were conducted routinely on the vacuum system to insure minimal leakage. Settings for the RF discharge power remained the same throughout providing the same forward power.

Using a signal averager program written by Dr. S. Heider, the computer controls the discharge (ON/OFF) and performs a host of functions concerning the data to include accumulation. When the discharge is on, the computer accumulates the signal and when the discharge is off, it subtracts the background signal with each having an accumulation time of about 7 seconds. This process is repeated twenty times for a total accumulation period of

about 5 minutes. Under steady conditions for the same wavelength region, at least three sets of data (minimum) were taken to insure reproducibility.

3.4.3 Procedures used to study Intensity Changes between 5790 Å and 6080 Å

Following observation of changes in Region A, the experimental setup was reconfigured by removing the lens to allow for a direct observation of changes across a wider region of the CO spectrum. Three different wavelength settings on the monochromator of 5840 Å, 5940 Å and 6040 Å provided for the study of the CO spectrum between 5790 Å and 6080 Å. With each spectrum of a 140 Å width at each setting, the three spectra were overlapped to provide the whole spectrum. This approach allowed for a more direct comparison of line intensity changes across the spectrum without the multiple scaling requirements that might be needed in assembling 51 runs, for example, if the spectra were each of only 18 Å wide. Matching three spectra using the available Assembler Program rather than some fifty spectra lessens the possibility by a considerable margin of scaling spectral intensities to a degree where relative intensity changes could be misinterpreted. The major drawback, as mentioned earlier, is the lesser spectral resolution which prevents resolving spectral lines at the rotational energy level.

The study of this region at the described spectral resolution concentrated on the effects of oxygen only on the carbon monoxide spectrum. Previous observations indicated that helium did not affect the relative change of intensity in the CO spectrum. This was expected since the first excited electronic state for helium is approximately twice the energy of the higher vibrational energy levels of ground state CO which are observed in this spectrum. Previous studies⁷⁻⁸ have shown that addition of helium

improves the thermal conductivity of the gas mixture lowering the rotational and vibrational temperatures. In turn, helium helps maintain a high electron temperature allowing for a high current density from the discharge to induce a relative higher excitation rate in the CO molecules.

Spectra of CO were taken at various pressures equal to and less than one Torr using the configuration for lesser resolution. Attempts at pressures above one Torr without the addition of oxygen seemed to create a chemical breakdown in the CO gas by the discharge. When the discharge was turned on, the laser light inside the glass tubing of the absorption cell appeared to be scattered from particulates forming in the gas. A brownish-black residue collected on the inside surfaces of the tubing near the electrodes. More about this phenomena will be discussed in the analysis section of this report.

In addition to CO spectra taken at various partial pressures of O_2 , spectra of pure O_2 were also taken at pressures ranging from 0.05 to 2 Torr. Comparisons of the pure CO spectra, pure O_2 spectra and mixed CO- O_2 spectra were made to analyze intensity changes.

Calibration of the spectra in terms of the assigned wavelengths was done through the use of a neon emission lamp. At each wavelength setting on the monochromator, channel numbers were assigned wavelengths from those established neon emission lines observed in that particular spectral region.

References

1. G. O. Brink, S. Spence and H.S. Lakkraju, *Optics. Comm.*, 32(1), 129 (1980).
2. G. O. Brink, *Optics Comm.*, 32 (1), 123 (1980).
3. H. Kogeliwik, E. Ippen, A. Diehes, C. Shank, "Astigmatically Compensated Cavities for CW Dye Lasers", *J. of Wuant. Mech.*, QE-8, 3, 373 (1972).
4. H. Holt, "Laser Intracavity Absorption", *Physical Review A*, 11, 12, 625 (1975).
5. K. Kim, "Dye Laser Intracavity Absorption Spectrum of the Hydrogen Molecule", Ph.D. thesis, SUNY/Buffalo, 1986.
6. A. Salih, "Dye Laser Intracavity Absorption Spectrum of Carbon Monoxide", Ph.D. thesis SUNY/Buffalo, 1986.
7. R. Schinke, G. Dierksen, "Vibration Relation of CO (n=1) in Collisions with He", *J. Chem. Phys.*, 83, 9, 4516 (1985).
8. R. Millikan, "Carbon Monoxide Vibrational Relaxation in Mixtures with Helium, Neon and Krypton", *J. Chem. Phys.*, 40, 9, 2594 (1963).

CHAPTER IV

RESULTS AND ANALYSIS

4.1. General:

The discussion in this chapter is divided into two sections. The first will address the intensity changes in Region A (5913-5923 Å) of the CO spectrum when helium and oxygen gases are added to carbon monoxide. The second section will discuss CO spectrum changes between 5790 Å and 6080 Å when only oxygen is added to CO. Analysis of these changes will include possible energy transfer mechanisms and chemical reaction processes involving carbon monoxide and oxygen. Considerable attention is devoted to the possibility of a resonant energy transfer between the upper vibrational levels of ground state CO and vibrational levels of the excited $C^3\Pi_g$ electronic state of O_2 .

4.2. Region A (5913-5923 Å) of Carbon Monoxide Spectrum:

At the higher resolution of 0.074 Å, analysis of relative intensity changes of the CO spectrum between Region A (5913-5923 Å) and adjacent regions (5923-5933 Å and 5908-5913 Å) was conducted. This interest was generated by Salih's report¹ that the intensity of the lines decreased in Region A when oxygen and helium were added. Of the assigned lines by Salih in Region A, most are from the (43-18), (38-12) and (37-11) bands of the $X^1\Sigma^+-A^1\Pi$, belonging to the Fourth Positive System. The greater contributions come from the (43-18) and (37-11) bands. At this resolution, the identification of the rotational spectrum in each band was made. Fig. 4.1 shows the pure CO spectrum (6 Torr) and the mixed gas spectrum (12 Torr

Fig. 4.1 - Salih's CO and Mixed Spectra between 5939 Å and 5910 Å.

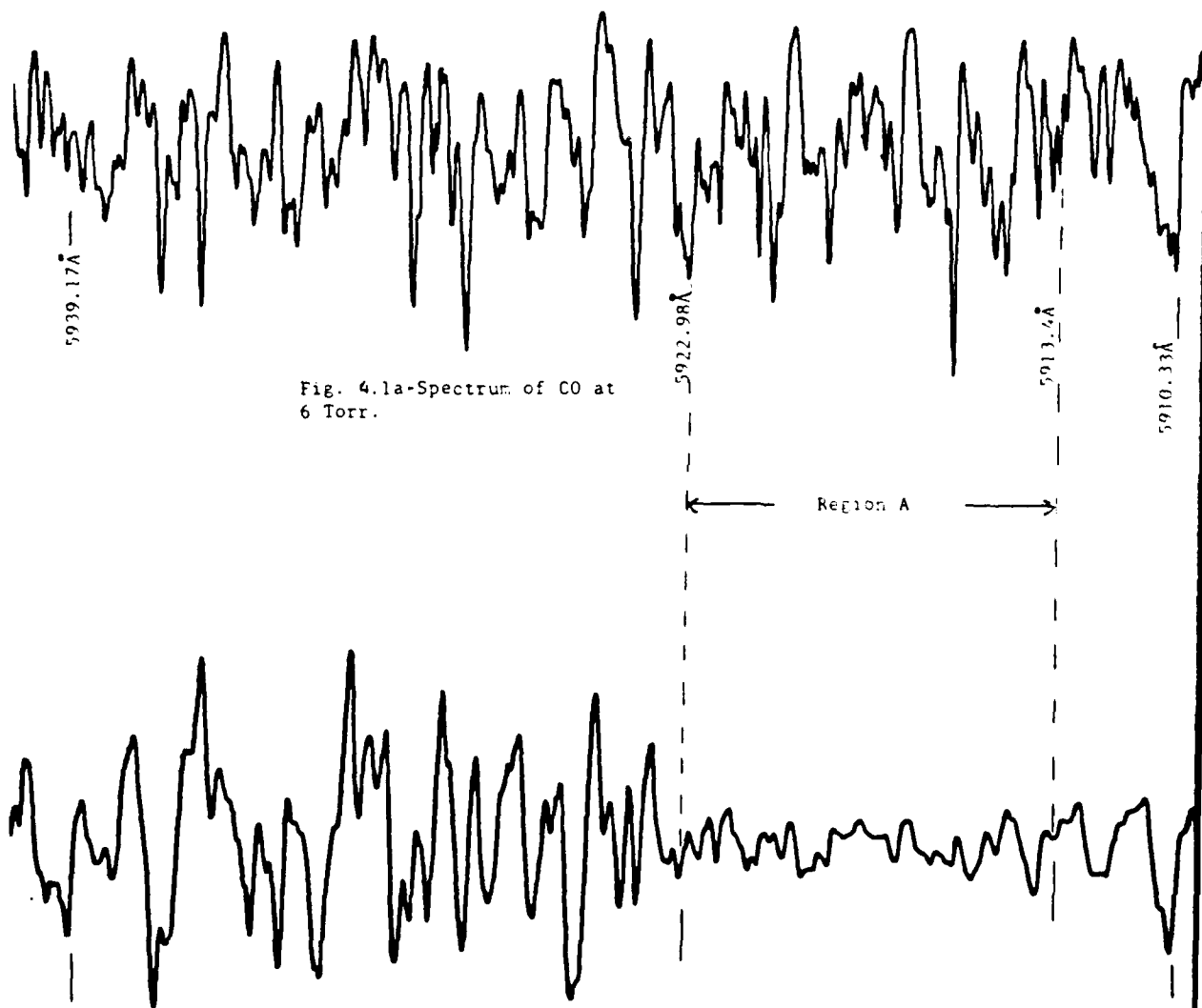


Fig. 4.1a-Spectrum of CO at 6 Torr.

Fig. 4.1b-Mixed He-CO-O₂ Spectrum taken at partial pressures of 12 Torr, 0.5 Torr and 0.1 Torr respectively.

He, 0.5 Torr CO and 0.1 Torr O₂) between 5939 Å and 5910 Å which was obtained from Salih's matched data. The section that is identified as Region A (Fig. 4.1b) positively indicates a decrease in intensity as compared to the left adjacent side outside of the designated region. Although not fully shown, a similar difference is observed between the right adjacent side and Region A. As a result, it appeared that the addition of the two gases were responsible for this relative intensity change.

Further examination of this region in the CO spectrum was conducted under similar conditions in this study. However, two experimental set-up changes were made which differed from Salih's work. First, an RF discharge system was used instead of a microwave discharge and secondly, for the mixed spectra, the gases were examined in a static, non-flow condition rather than the flow. Although those changes may alter the line intensities of the pure and mixed spectra, the effects of adding both gases to the CO should still remain.

Fig. 4.2 shows the pure CO spectrum (1 Torr) and the mixed spectrum (6 Torr He, 0.25 Torr CO and 0.05 Torr O₂) between 5934 Å and 5910 Å as taken in this experiment. The ratio of gas pressures for the mixed spectrum corresponds to those in Salih's experiment. The results differ from his in that the decrease of relative intensities within Region A is not seen here. In contrast, it reveals that the addition of He and O₂ has enhanced the intensities across the entire section of this spectrum in almost uniform fashion. The lines in Region A have not been depressed by the addition of the gases as seen in Fig. 4.1. Close examination of the absorption lines does show the same lines as seen in Salih's spectra but the magnitude of the

Fig. 4.2. - CO and Mixed Spectra from present work between 5934 Å and 5910 Å.

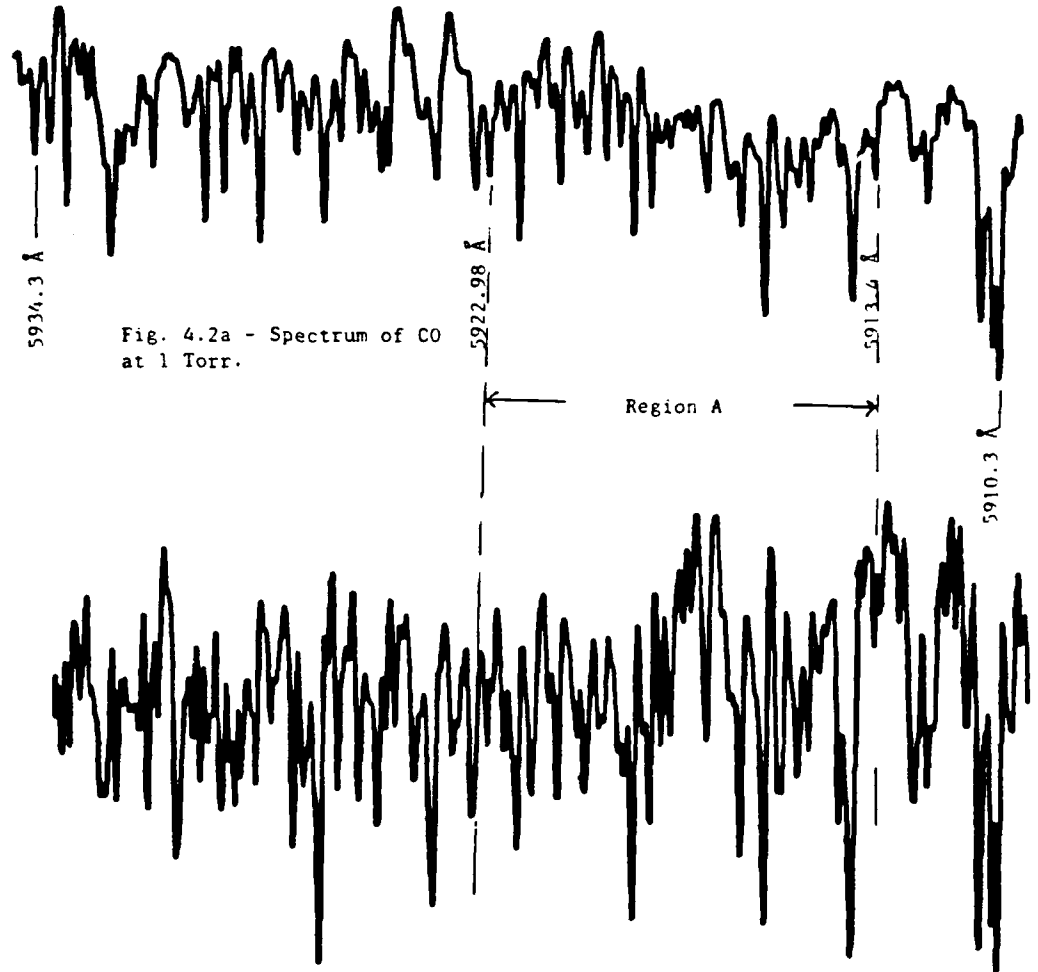


Fig. 4.2a - Spectrum of CO at 1 Torr.

Fig. 4.2b - Mixed He-CO-O₂ Spectrum taken at partial pressures of 6 Torr, 0.25 Torr and 0.05 Torr respectively.

various lines has changed. Equipment modifications such as the different discharge system may account for this variation.

The spectra in Fig. 4.2 represents two 18 Å sections of spectrum with each spectrum covering more than one-half (11 Å) of the same spectral region. Both sections were matched and then plotted as shown. Scaling of the data in either section when matched was not significant.

The probability of resonant energy transfer between any three of the ground state vibrational levels ($v=43,38$ and 37) found in this region for CO with vibrational levels of excited electronic states in oxygen or helium is unlikely. As previously mentioned, the first excited electronic state for helium has an energy value of 146365 cm^{-1} , about twice the energy than those upper vibrational levels of ground state CO. Because the energy defect is large, the probability of energy exchange is extremely small. As for energy transfer between CO and O_2 , the probability is much greater but still unlikely for those vibrational levels of CO assigned to the bands in Region A of the spectrum. If we are to examine the energies in Table 2.1, the probability for V-V energy transfer between the upper vibrational levels of the CO ground electronic state and the vibrational levels of the excited electronic states, $\text{C}^3\Pi_g$ and $\text{d}^1\Pi_g$, of O_2 is small due to significant mismatch of energy levels. Vibrational energy levels, $v=38$ and $37 \text{ X}^1\Sigma$ of CO are more than 1000 cm^{-1} below any of the vibrational levels of the $\text{C}^3\Pi_g$ and $\text{d}^1\Pi_g$ states in oxygen. There is also a sizeable energy difference between $v=43$ of $\text{X}^1\Sigma$ CO and $v=1$ of $\text{C}^3\Pi_g$ of O_2 . With these upper vibrational levels of CO as the major contributors to the bands in Region A, a reduced population density at these levels due to V-V transfer with excited O_2 seems

improbable. Other energy transfer mechanisms are possible but are unlikely to affect only those transition bands within Region A. Further discussion will follow later on these other mechanisms.

Despite the above argument, there could exist a small probability of energy transfer between vibrational levels of CO and O₂ based on the inexact determination of the energy values for those vibrational levels of the C³Π_g state in O₂. Limits were established on the energy measurements of the band origins of these levels by Huebner² and Cartwright³ during their investigation and those values in Table 2.1 are the averaged figures. At the extreme limit, an energy spacing of 750 cm⁻¹ exists between v=43 (X¹Σ) of CO and v=2 (C³Π_g) of O₂ which may provide a possible avenue for energy exchange. Even though this possibility is still unlikely since the v=42 level for CO is nearer to the v=2 (C³Π_g) level for O₂, further examination of Region A was warranted before disclaiming any relative intensity changes.

The mixed spectra of CO were taken with and without helium over various pressures of O₂ for Region A. Spectral data were collected for mixed carbon monoxide at 0.25 Torr and helium at 6 Torr with changes in partial pressure of O₂ between 0.01 and 0.15 Torr. Partial pressures for each gas were similar in ratio to those measurements taken by Salih. Additional data were also obtained without helium in the mixture with various partial pressures of O₂ between 0.01 and 0.5 Torr keeping constant the partial pressure of CO at 1 Torr. The inert nature of helium when mixed with CO and our developed interest on the effects from oxygen alone were reasons for also examining the

spectra without helium. It should be noted that helium, in addition of acting as an convective coolant for the system, has been shown to raise the value of current in a discharge to help maintain a high excitation rate. Fig. 4.3 depicts the pure CO spectrum and the mixed CO-He spectrum (0.25 Torr: 6 Torr) for the same spectral region (5934-5910 Å). Corresponding lines from each spectrum were easily identifiable and relative intensity changes are not observed from the addition of helium. The addition of helium increased the intensities across the entire region and supports the claim for improved excitation rate.

Selected lines were chosen within Region A and adjacent sections of the spectrum to examine relative intensity changes. Sixty-nine separate data runs that included twenty-five of these selected lines across the spectrum were analyzed and compared for intensity differences. Plots of intensity ratio ($I_{\text{MIX}}/I_{\text{CO} + \text{He}}$ and $I_{\text{MIX}}/I_{\text{CO}}$) versus partial pressure of O_2 were made for each selected peak to identify the direction of intensity changes with the addition of oxygen. Fig. 4.4 shows a series of spectra between 5932 Å and 5915 Å with oxygen at pressures of 0.05, 0.10 and 0.25 Torr added to carbon monoxide alone at 1 Torr. A general inspection of the spectra indicates a slight overall increase of intensity throughout the spectral region as more oxygen is added to the mixture. Fig. 4.5 shows spectra with similar additions of oxygen but for a wider region of the spectrum between 5932 Å and 5910 Å.

Measurement of any one line of the various spectra was difficult at best due to the closeness of adjacent lines. Establishing a standard reference for each peak to measure relative changes at different conditions was necessary. However, even with the most care, slight changes in the position of that reference by the very nature of the intensity changes in

Fig. 4.3 - CO and mixed (CO + He) Spectra between 5934 Å and 5910 Å.

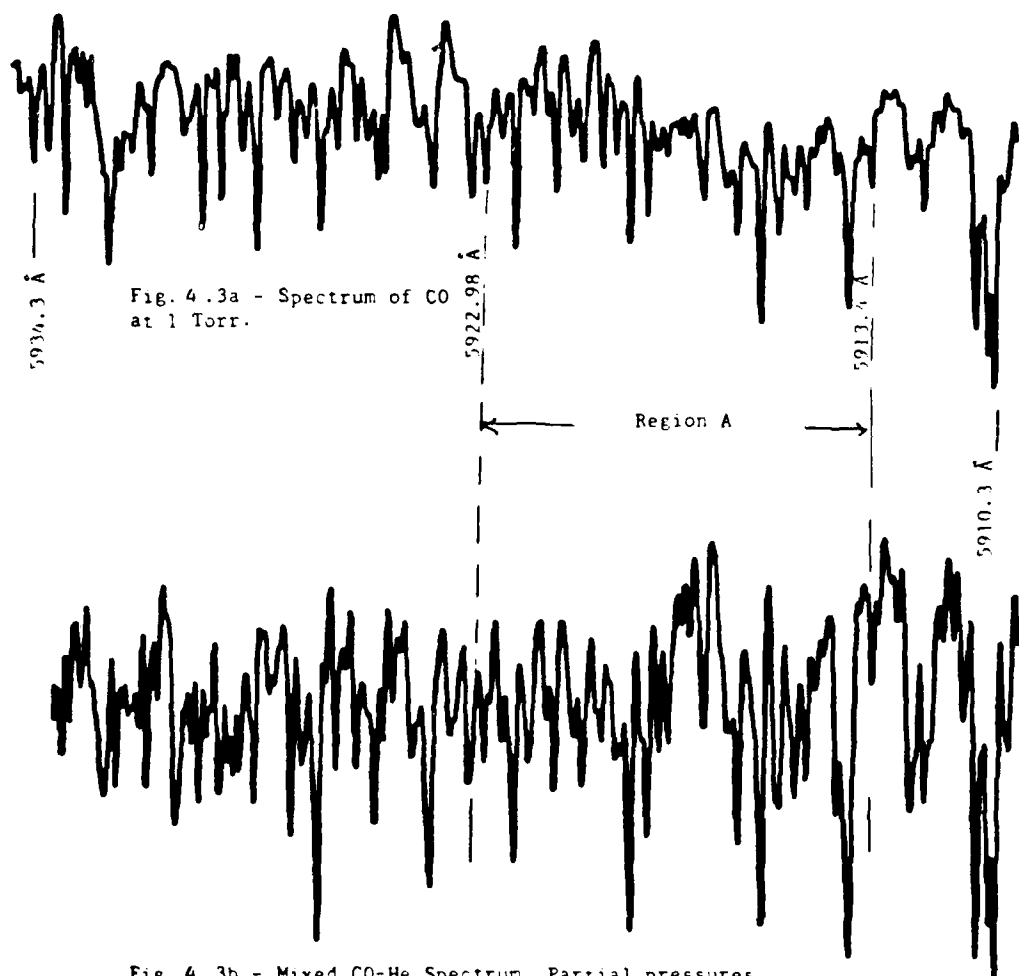


Fig. 4.3a - Spectrum of CO at 1 Torr.

Fig. 4.3b - Mixed CO-He Spectrum. Partial pressures for carbon monoxide and helium were taken at 0.25 Torr and 6 Torr respectively.

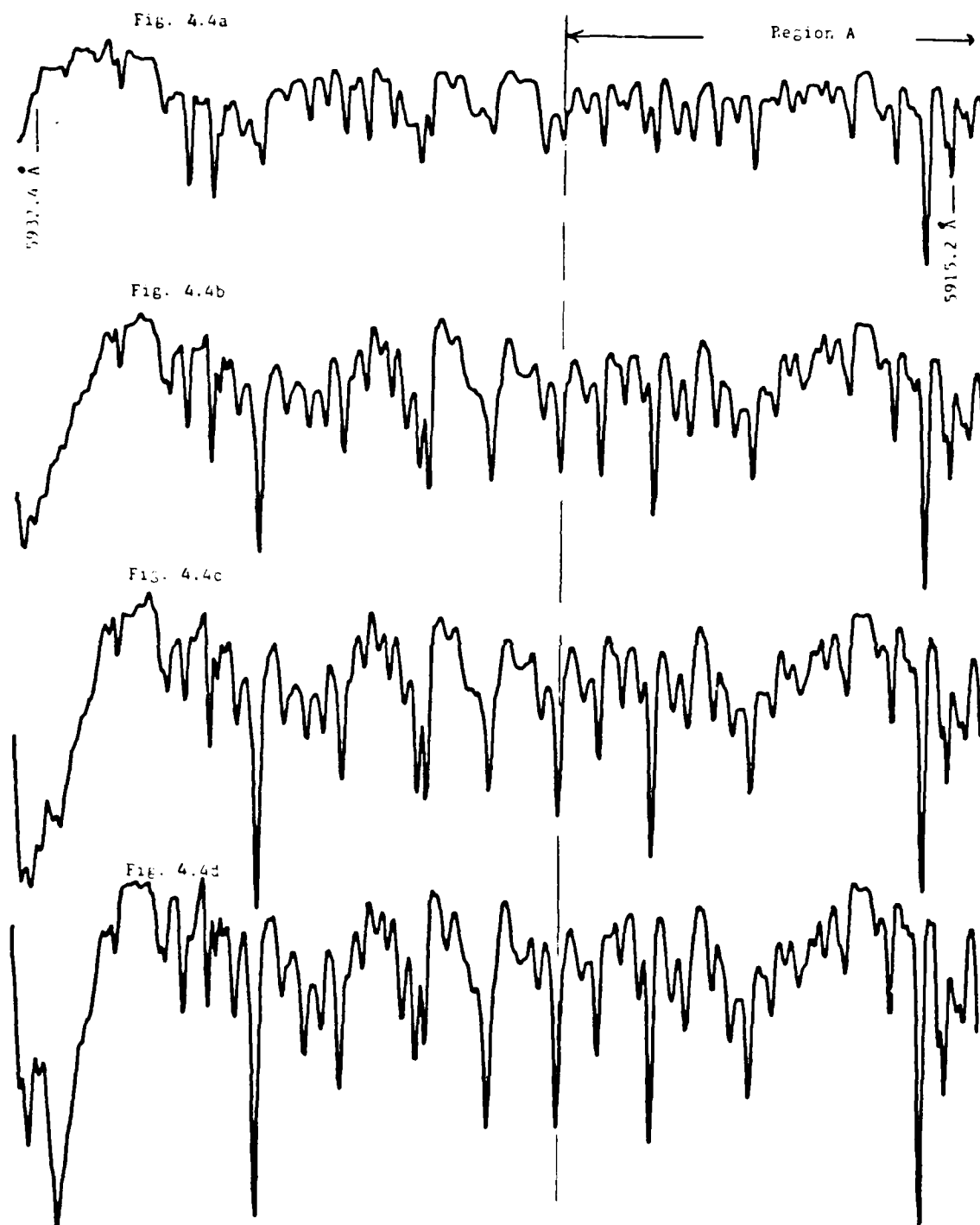


Fig. 4.4a-d - Spectrum of CO at 1 Torr and mixed CO-O₂ spectra with O₂ at partial pressures of 0.05 Torr, 0.1 Torr and 0.25 Torr respectively.

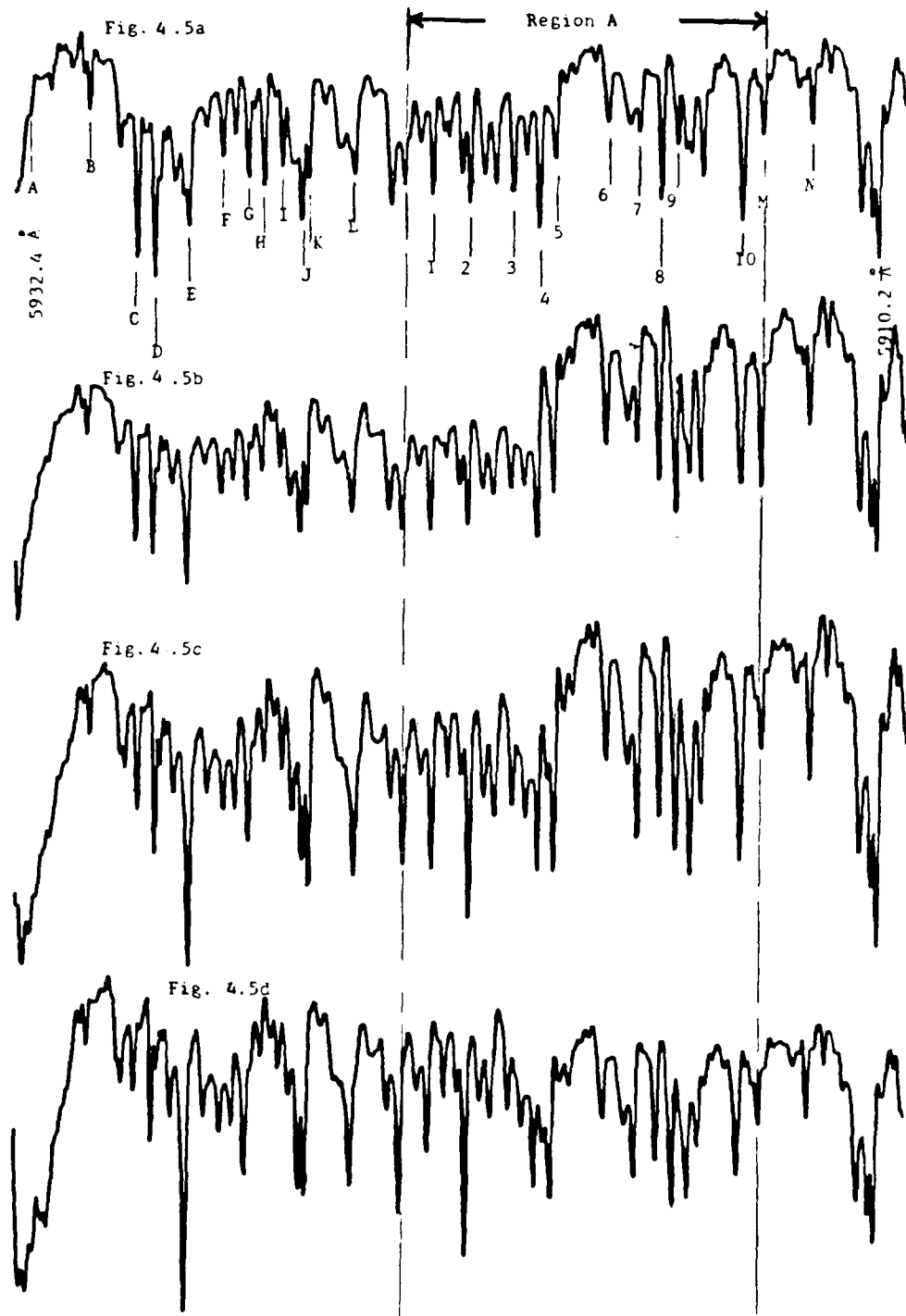


Fig. 4.5a-d - Spectrum of CO at 1 Torr and mixed CO-O₂ spectra with O₂ at partial pressures at 0.01 Torr, 0.05 Torr and 0.1 Torr, respectively, between 5932 Å and 5910 Å.

each line caused deviations in obtaining absolute changes. Whether the coolant effect from helium played a role or not, data was more consistent with the change of oxygen in a CO-He mix than with just CO alone.

Absorption lines that were specifically measured to determine relative intensity changes are underscored with an identifying number or letter in Fig. 4.5a. Appendix A contains the data plots of the absorption lines which depict the intensity ratio with CO and He at 0.25 Torr and 6 Torr, respectively, over the change of O_2 pressure between 5 and 150 millitorr. Appendix B shows the plots of the same lines for CO at 1 Torr but without helium in the mixture. Changes in O_2 pressure ranged between 0.01 and up to 0.5 Torr. The lettered lines indicate those outside Region A and the numbered ones are for those inside the region. The lines were selected based on their prominence in the region which left some to be unassigned.

The most important result from examination of the mixed spectra is that no relative intensity change between Region A and its adjacent regions was observed. Of the total spectra, there was not one mixed spectrum to indicate a relative intensity decrease in Region A. Elimination of helium in the mixture appears to have made no difference in regard to this effect. The data plots for the helium mixture in Appendix A were found to be relatively linear and even over an increase of oxygen in the region of pressure between 5 and 150 millitorr. Measurements of intensity changes were more consistent with the mixed spectra which included helium. Helium is known to dominate in V-T energy transfer processes in CO and O_2 mixtures and thus might be a contributing factor towards the more consistent data that is realized in the helium mixtures. The changes of the ten absorption peaks inside Region A generally indicated a slight increase of intensity as the

partial pressure of O_2 was raised. This was especially more true for those peaks of the mixed spectra that excluded helium from the mixture. For the absorption peaks outside Region A, the changes were less consistent. Numerous lines showed a decrease while others showed an increase with the addition of oxygen. The overall effect of CO (with or without helium at 6 Torr) with the addition of oxygen between 0.01 and 0.5 Torr appears to be a general increase of intensity across this spectral region not limited to only Region A. There is an absence of any localized change, either of enhancement or suppression, between 5910 Å and 5934 Å when oxygen is added to carbon monoxide. The positions of the absorption peaks for the CO-He spectra along the spectrum at the partial pressures between 0.05 and 0.15 Torr of O_2 did not vary from those observed in the pure CO spectrum. This observation is important since our goal is to examine changes to the CO spectrum and not mistakenly interpret changes due to the overlapping effects of the oxygen spectrum in this region. The mixed spectra after comparing it with the CO and O_2 spectra, resembles the CO spectrum line by line at these partial pressures for O_2 .

Unsuccessful attempts were made to display the pure CO spectrum by subtracting the oxygen spectrum at these partial pressures from the mixed spectrum. Absolute intensities for pure O_2 at pressures between 0.1 Torr and 0.15 Torr were almost twice as large as those observed in the mixed spectrum where the total gas pressure was above 1 Torr. At higher pressures the quenching effect due to the increased intermolecular collisions results in lower intensities. Therefore, subtracting the higher intensity spectrum of O_2 from the mixed spectrum resulted in data that did not resemble the CO spectrum.

At partial pressures of O_2 greater than 0.25 Torr with CO at 1 Torr, evidence of overlapping effects was more noticeable since the change of line positions as compared to those lines of the pure CO spectrum showed greater disparity. This would support the slightly higher rate of inconsistency which is seen in the data at higher partial pressures of O_2 for some peaks (see Appendix B; Peaks 3,5,E,H,M).

A broad inspection of Region A and adjacent regions was made by lowering the spectral resolution and examining the spectrum over a wider section as earlier described. Fig. 4.6 again shows the pure CO spectrum at 1 Torr between 5890 Å and 6030 Å and the changes of the spectrum as oxygen is added with partial pressures of 0.1, 0.5 and 1.0 Torr. The absorption lines of the mixed spectrum with added oxygen at 1 Torr for Region A have significantly increased in intensity by almost three fold. These lines in this region are highly dominated by those of O_2 at partial pressures greater than 0.5 Torr as our discussion in the next section will reveal.

4.3. Possible Resonance Energy Transfer between $v=40 X^1\Sigma$ of CO and $v=0 C^3\Pi_g$ of O_2

Since the investigation of Region A of the CO spectrum did not indicate a relative intensity change with its adjacent regions, our examination on the effects of oxygen on the CO spectrum was expanded to between 5790 Å and 6080 Å. This was the entire region of the spectrum which could be observed using the dye laser under existing conditions. The detection equipment was configured for a lesser spectral resolution but provided a 140 Å width spectrum which enabled easier observation of intensity differences.

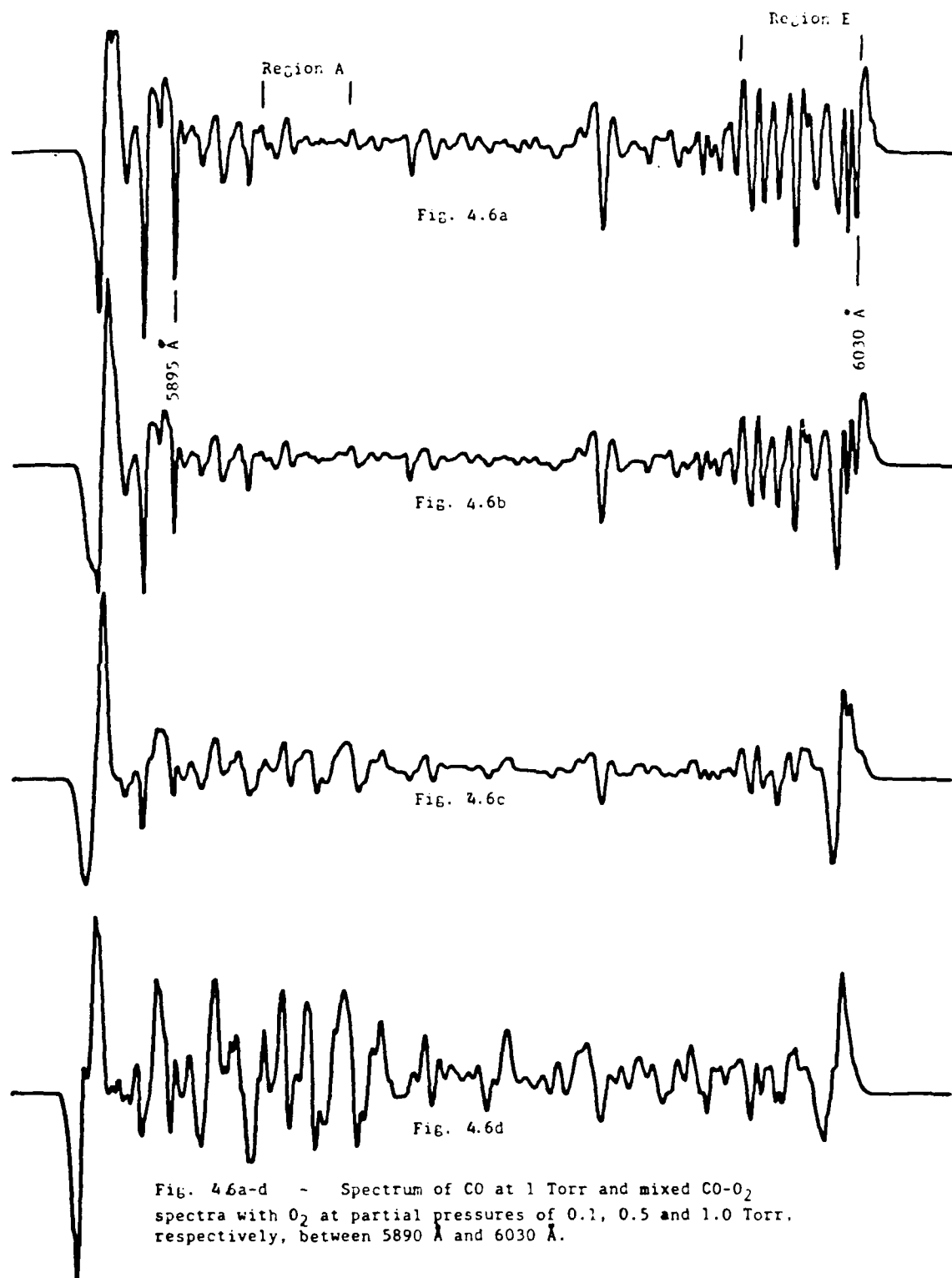


Fig. 4.6a-d - Spectrum of CO at 1 Torr and mixed CO-O₂ spectra with O₂ at partial pressures of 0.1, 0.5 and 1.0 Torr, respectively, between 5890 Å and 6030 Å.

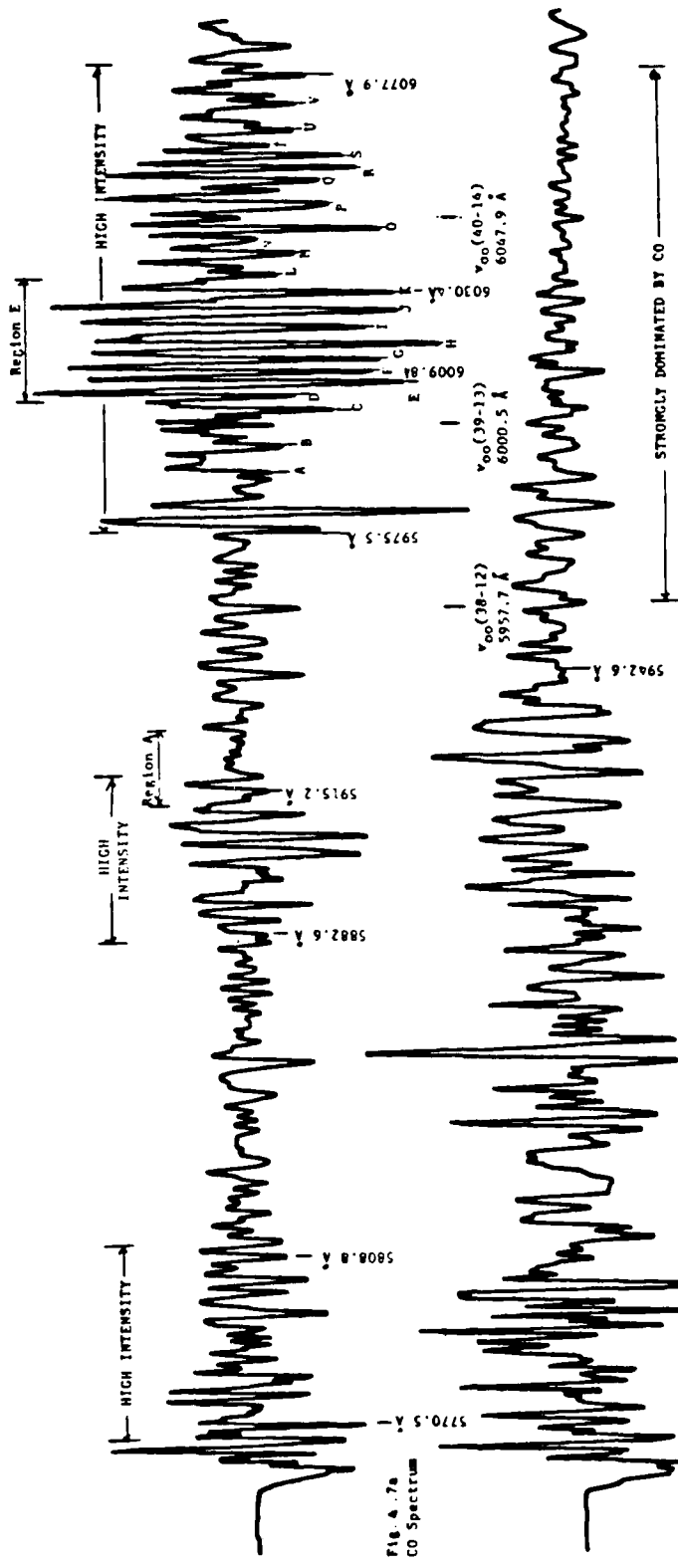


Fig. 4.7a
CO Spectrum

Fig. 4.7b
Mixed Spectrum

Fig. 4.7c
O₂ Spectrum

Fig. 4.7a-c - Spectra of CO and O₂ taken at 1 Torr each and the Spectrum of mixed CO and O₂ in the center taken with each gas at 1 Torr.

pure CO and O₂ spectra making contributions from either indistinguishable. Lines at the far right of the mixed spectrum, 6010 Å and greater, exhibited stronger dominance by CO.

The pure O₂ spectrum, Fig. 4.7c, possesses intensities between 5770 Å at the left end and 5980 Å of almost three to four times greater than those of pure CO. At about 6020 Å and greater, the relative intensity of the O₂ spectrum decreases to almost equal to those intensities shown by CO in the same region. Comparisons among the three spectra in Fig. 4.7 regarding line intensity differences is somewhat deceiving since each is plotted based on its own maximum intensity count. Although the intensities of the higher wavelength region of O₂ appears less than that of the CO spectrum, the relatively high intensity region at the lower wavelength region in the O₂ spectrum has caused the relative scaling down of intensities throughout, to include the higher wavelength region. Therefore, the difference in magnitude of intensities between CO and O₂ for Region E is not as great as it appears in the plots.

Even with the above considerations about intensity differences, analysis of the relative high intensity lines in the CO spectrum between 6000 Å and 6060 Å shows an intensity decrease as oxygen is added. In Fig. 4.6, on the far right of the spectrum which is identified as Region E, these line intensities can be seen to decrease as oxygen is added at partial pressures of 0.1, 0.5 and 1 Torr. Measurement of the intensity changes of the peaks in this region positively indicate a decrease over this range of added pressures of O₂. Appendix C contains the data plots of the absorption lines in Region E and adjacent regions. The plots depict the intensity

ratio ($I_{\text{MIX}}/I_{\text{CO}}$) with CO at 1 Torr over the change of O_2 pressure between 0.3 Torr and 1.0 Torr. If the intensity of these lines decrease with the addition of O_2 as the data seems to indicate, it would mean that the population densities of the upper vibrational levels for ground state CO, as identified by the transition bands in the region, would also decrease. This would suggest a possible energy exchange from these upper vibrational levels to either translational or internal energy of oxygen.

Further investigation was undertaken to determine if the suppression of lines in the CO spectrum was not the result of overlapping effects from the O_2 spectrum in the observed mixed spectrum. In our previous discussion of Region A, attempts of subtracting out the oxygen spectrum from the mixed spectrum to display the pure CO spectrum proved unsuccessful. Similar attempts were made at this lower resolution for the entire observed spectral region. Again, this did not provide a spectrum that would provide any useful information about intensity changes for lines in the CO spectrum itself. However, the spectra of CO and O_2 at 1 Torr each were added and compared to the mixed spectra of both gases at the same pressures. Fig. 4.8 shows both spectra where each was scaled and plotted relative to the peak with the highest data count. Similarities of lines between the two spectra can be easily seen especially on the left side in the region between 5770 Å and 5960 Å. This was the region of the mixed spectrum where the lines were strongly dominated by O_2 . On the right side of spectrum from 5960 Å to 6080 Å, lines of the mixed spectrum were found to be more closely associated with those of the CO spectrum. Comparisons of this same region between both spectra in Fig. 4.8 show line shapes to be similar but the overall relative intensities to be higher in the added spectrum than in the mixed spectrum.



Fig. 4.8a
Mixed CO-O₂ Spectrum at partial pressures
of 1 Torr each.

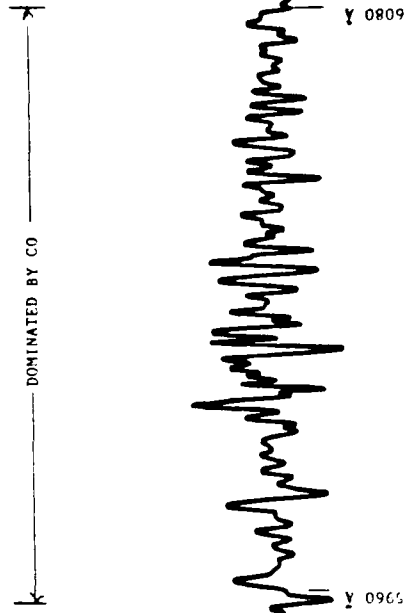


Fig. 4.8b
Summed Spectra of CO and O₂ at 1 Torr each.

Attention was given to avoid some erroneous scaling factor which might arbitrarily change the relative intensity of this region with respect to the rest of the spectrum. If the lines in this region between 5960 Å and 6080 Å, especially in the vicinity of Region E, are strongly CO dominated lines and the relative intensity difference in Fig. 4.8 between the two spectra is accurate, then there is good reason to suggest a possible energy exchange between CO and O₂.

Resonance energy transfer between vibrational levels of both excited molecules during collisions is one possible means for the energy to decrease from the upper vibrational levels in CO. The efficiency of such a transfer is dependent on the electronic states and the vibrational and rotational levels of each molecule. For CO, in the region between 6000 Å and 6060 Å transition band contributions are largely from the vibrational levels v=39 and v=40 of the X¹Σ ground state. If we reexamine Table 2-1, the v=0 vibrational level of oxygen's excited C³Π_g state (a lower Rydberg state for the molecule) matches fairly close with the v=40 X¹Σ level of the CO with an energy defect of about 150 cm⁻¹. This difference could actually be less since the assigned energies for these vibrational levels of the C³Π_g state are only approximate.

A factor to be considered regarding the probability of transitions from collisional effects of two such molecules is the difference in multiplicity of both interacting electronic states. There is little to be found in literature about collisional dynamics involving a singlet ground electronic state such as the one in CO and an excited triplet electronic state from another molecule such as O₂. Our reference to the Krönig's selection rules

states that such transitions with different multiplicities are forbidden. For molecular collisions, this restriction is lessened allowing transitions from singlet to triplet and vice versa. The square of the matrix element coupling initial and final states, multiplied by the number of states per energy interval is proportional to the probability of such transitions per unit time. This is to assume that the energy for deexcitation of CO equals the energy for excitation of O_2 ; that is for which $\Delta E=0$. The matrix element could certainly be an electric dipole matrix element where a dipole-dipole interaction could induce near-resonant V-V transfer as suggested by Mahan⁵. In terms of the first-order Born approximation, the probability for a transition is the highest at $\Delta E=0$, exact resonance, and decreases rapidly with increasing ΔE . Therefore, the transition probability due to energy transfer between vibrational levels $v=40$ of $X^1\Sigma$ CO and $v=0$ of $C^3\Pi_g$ O_2 may be strong.

The likelihood of being able to identify a transition band in the O_2 spectrum for which the $C^3\Pi_g$ electronic state is the lower state is very small. Intensity changes of the vibrational bands originating from this state over varied partial pressures of CO and O_2 could provide additional information about the possible resonance energy exchange process between the two molecules. Since our system consists of a weak plasma, the transitions in the O_2 spectrum most likely originate from the ground electronic state, the $X^3\Sigma$ state. There are several transition bands possible in this spectral region of O_2 that could have initial states at higher energy levels than ground state. However, such transitions would be so weak in comparison to

the ground state transitions that observation of such lines in the O_2 spectrum is highly improbable. One such band in the O_2 spectrum includes the $C^3\Pi_g$ state as the initial state in the band $(1-0) C^3\Pi_g \rightarrow E^3\Sigma_u^-$ with a calculated band origin of 5796 Å. Overlapping effects from other transitions in the same region and the likely weakness of this transition would make observation of the $C^3\Pi_g$ state most unlikely.

Further comparisons on Table 2.1 indicate another possible resonance energy transfer between $v=45 X^1\Sigma$ of CO and $v=3 C^3\Pi_g$ of O_2 with an energy defect of 96 cm^{-1} . The origin for the $(45-20) X^1\Sigma-A^1\Pi$ band is 6075.6 Å, at the far right end of Fig. 4.7a, where complete observation of the assigned band cannot be made. It is important to note that Brechignac⁵ using a CO-He plasma discharge, reported that the population densities at vibrational levels higher than $v=40$ for the ground state decrease by almost one order of magnitude. In addition, Millikan⁶ has measured the cross section for V-T relaxation of CO by O_2 and found it to be quite high. The probability of V-T relaxation is proportional to the vibrational quantum number, and would thus be expected to be more noticeable for the higher lying vibrational levels of CO. Although V-V relaxation is usually rapid compared to V-T, both processes become comparable at these higher vibrational levels. Even though intensities did decrease with added oxygen in the region of the $(45-20)$ band, other competing mechanisms may contribute to the decrease in intensity.

An attempt was made to observe the atmospheric band $(X^3\Sigma_g^- \rightarrow ^1\Sigma_g^+)$ of O_2 using the ICA technique without using the RF discharge. Despite the

relative high sensitivity of ICA, lines from this band could not be observed. If it were otherwise, such a spectrum may have allowed us to study the excitation of ground state oxygen and to expand further on possible energy transfer mechanisms.

One major difficulty in the analysis of the intensity changes was to simply be able to observe changes of those lines of interest. Within this entire CO spectral region, lines from triplet state transitions overlap these singlet state transition bands which commanded our attention in this study. This "dirty" spectrum made it extremely difficult to interpret actual intensity changes because of the influence of these other lines. In CO, there are transitions which originate from the $a^3\Pi$ state to higher electronic states (i.e. (4-0) $a^3\Pi \rightarrow d^3\Delta_1$ band) which may significantly affect interpretation of intensity changes of the singlet transitions. Analysis of the pure CO spectrum is difficult for this reason. The spectrum becomes even more complicated when O_2 is added and analysis of the mixed spectrum must be made. Overlapping effects increase in the mixed spectrum which make analysis of intensity changes of particular transition bands additionally difficult.

Millikan⁶ in his report on CO relaxation reported that CO- O_2 collisions showed an anomalous efficiency in causing vibrational relaxation. The degree of chemical affinity between both molecules plays an important role in such energy transfer processes. The effect of the discharge will be to excite a small percentage of the gas into species where reactions with other species occur more easily. For CO alone without oxygen, it was observed at pressures greater than 1 Torr that brownish-black deposits

formed on the wall of the absorption cell. Bergman et. al.⁷ reported a similar experience using a discharge and subsequently discovered that such a deposit was a mixture of polymeric forms of carbon suboxide C_3O_2 . The basis for such an observation stems from the following reactions:

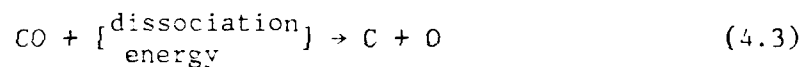


where carbon atoms formed in this reaction react further with $CO(v \approx 0)$ to form carbon suboxide.



It is believed that such a sequence resulting in CO_2 and C_3O_2 as the stable products is the dominant reaction.

Osgood⁸ in his discussion of excitation of CO in CO lasers states that the following reactions in the excited plasma are possible:



Since our system is a weak plasma, the average electron energy necessary for CO dissociation will be small. However, Phelps⁹ has shown that direct electron impact excitation of CO has a large cross section. Therefore, the possibility for some dissociation of the CO exists as indicated by the first mechanism (eq. 4.3). Evidence of O_3 as a product of He-CO- O_2 gas discharges has been noted previously⁸. It is conceivable according to the second and third mechanisms (eqs. 4.4 & 4.5) that addition of O_2 in the system may provide a greater concentration of CO and ultimately compete with the dissociation effect of the first mechanism. The third reaction (eq. 4.5)

may also be one possibility as to why the addition of O_2 in the pure CO gas seemed to decrease or eliminate the deposit buildup of the alleged carbon substance on the walls of the absorption cell.

It would appear that the role of O_2 in this system acts not only as a possible collision partner for energy exchange with CO or vice versa, but that the degree of chemical affinity between each molecule and with those products formed in reaction mechanisms contribute to the overall energy transfer in the system. The energy transfer processes involved in these reaction mechanisms could influence the possible V-V energy exchange processes between CO and O_2 .

REFERENCES

1. A. Salih, "Dye Laser Intracavity Absorption Spectrum of Carbon Monoxide", Ph.D. Thesis, SUNY at Buffalo, 1986.
2. R. H. Huebner, R. J. Celotta, S. R. Mickzarek, C. E. Kuyatt, "Apparent Oscillator Strengths for Molecular Oxygen Derived from Electron Energy-Loss Measurements", *Journal of Chem. Physics*, Vol. 63, 1, 241 (1975).
3. D. C. Cartwright, W. F. Hunt, W. Williams, S. Trajmr, W. A. Goddard, "Theoretical and Experimental (Electron-Impact) Studies of the Low-Lying Rydberg States in O₂", *Physical Review A*, Vol. 8, 5, 2436 (1973).
4. B. H. Mahan, "Resonant Transfer of Vibrational Energy in Molecular Collisions", *Journal of Chem. Physics*, Vol. 46, 1, 98 (1967).
5. P. Brechignac, J. P. Martin, G. Taieb, "Small-Signal Gain Measurements and Vibrational Distribuion in CO", *Journal of Quantum Elect.*, Vol. QE-10, 10, 797 (1974).
6. R. C. Millikan, "Vibrational Fluorescence of Carbon Monoxide", *Journal of Chem. Physics*, Vol. 38, 12, 2855 (1963).
7. R. C. Bergman, G. F. Homicz, J. W. Rich, G. L. Wolk, "¹³C and ¹⁸O Isotope Enrichment by Vibrational Energy Exchange Pumping of CO", *Journal of Chem Physics*, Vol. 78, 3, 1281 (1983).
8. E. M. Osgood, W. C. Eppers, E. R. Nichols, "An Investigation of the High-Power CO Laser", *Journal of Quantum Electronics*, Vol. QE-6, 3, 145 (1970).
9. R. D. Hake, A.V. Phelps, "Momentum-Transfer and Inelastic-Collision Cross Sections for Electronics of O₂-CO, and CO", *Physics Review*, Vol. 141, 71 (1966).

CHAPTER V

CONCLUSION

The purpose of this study was to investigate possible resonance energy transfer mechanisms between carbon monoxide and oxygen in a radio frequency (rf) excited plasma at low densities using the dye laser intracavity absorption technique (ICA). Molecular absorption spectra of carbon monoxide and CO-O₂-He mixtures in the optical region between 5790 Å and 6080 Å were investigated to identify intensity changes in the CO spectrum as the result of adding oxygen and helium. A previous study reported an anomalous effect of either enhancement or suppression of lines intensities across this region of the CO spectrum from the addition of these gases. One small region, Region A (5913-5923 Å) was selected for further study where suppression of lines was indicated. Comparisons of the pure CO spectrum with the mixed-gas spectra at various partial pressures of O₂ were made to measure intensity changes of selected lines. A similar procedure was taken under lesser spectral resolution to examine changes in the CO spectrum across a greater optical region.

Transition bands from the Fourth Positive System ($X^1\Sigma-A^1\Pi$) of CO have been assigned in this spectral region where the initial states are the upper vibrational levels ($v=26$ to 46) of the ground electronic state. Coinciding at similar energies are two excited electronic states for oxygen, the $C^3\Pi_g$ and $d^1\Pi_g$ states. Both have vibrational levels which match relatively closely in energy with those of the upper vibrational levels of ground state CO. Contrarily, a large energy defect of approximately $80,000\text{ cm}^{-1}$ exists

between the upper vibrational levels of ground state CO and the first excited electronic state of helium. As a result, the most likely case for resonance energy exchange would be between CO and O₂. Possibilities of V-V and V-E energy transfer between both molecular systems were examined.

Results on Region A did not reveal an anomalous behavior in regard to adjacent regions of the CO spectrum as oxygen was added. Suppression of lines in this region was not observed as was earlier reported by Salih. Spectra of pure CO and mixed CO and He were analyzed. Changes of increased intensity were observed when oxygen was added to pure CO and mixed CO and He. Pressure ratios of two to one of CO and O₂, respectively, showed that the line positions of the mixed spectra matched closely to those of the pure CO spectrum. This would indicate that the observed lines in the mixed spectra strongly represent those of the pure CO. It was also observed that the intensity of lines of the mixed spectra in relation to the pure CO spectrum generally increased despite some exceptions as discovered in the selected line analysis for this region. Less consistent data regarding line intensities were obtained from mixed spectra that did not include helium in the gas mixture. Some lines which showed exception to the general intensity increase remained either even or showed a slight decrease. However, these effects were random and did not extend consistently across any one section of the spectrum.

Assigned bands in Region A are largely contributed by the vibrational levels $v=43$, 38 and 37 of ground state CO. Except for $v=43$, the energies of the other two levels lie more than 1000 cm^{-1} below any of the vibrational energy levels of the two aforementioned excited electronic states in oxygen. This large energy defect makes resonance energy transfer at this level

between both molecules unlikely. Even $v=43$ for CO has an energy spacing of 750 cm^{-1} from the $(v=2)\text{ C}^3\Pi_g$ state of O_2 which makes it improbable that energy would transfer to oxygen at that level. Therefore, the suppression of lines in this region for that reason would seem unlikely. In further support of this argument, earlier discharge excitation experiments on CO alone have shown a significant population decrease for ground state vibrational levels higher than 40. This would suggest that oxygen does not play an important role in the population decrease of vibrational levels of 40 or greater and therefore limiting the probability of resonance energy transfer at the $v=43$ level.

The general increase of line intensities when oxygen was added could be explained by the following: 1) addition of O_2 results in the conversion of some of the excess carbon atoms into CO, and 2) addition of O_2 lowers the average electron energy to the point where excitation of CO is favored (since O_2 has a lower ionization potential than either CO or He).

Observation of the CO spectrum in the entire optical region ($5790\text{-}6080\text{ \AA}$) revealed a relative high intensity region between 6000 \AA and 6060 \AA . Transition bands whose initial states are $v=39$ and $v=40$ of ground state CO contribute largely to the lines in that region. Contrary to Region A, the addition of oxygen suppressed the intensities throughout the 6000 \AA to 6060 \AA region designated as Region E. Lines of the mixed spectrum of 1 Torr CO and 1 Torr O_2 correlated closely to those of the pure CO spectrum at 1 Torr even though lines from the oxygen spectrum overlapped at numerous places. The $v=40$ state of CO matches closely to the $v=0\text{ C}^3\Pi_g$ state of O_2 with an energy defect of approximately 150 cm^{-1} . This would provide a

possible avenue for energy to flow between CO and O₂. However, this resonant energy transfer mechanism between vibration levels could not be confirmed since a transition band with the $v=0$ C³Π_g state as a lower state could not be identified in the O₂ spectrum for this spectral region. If such a band could be observed, an increase in intensity over the same change of conditions could have supported V-V and V-E energy transfer.

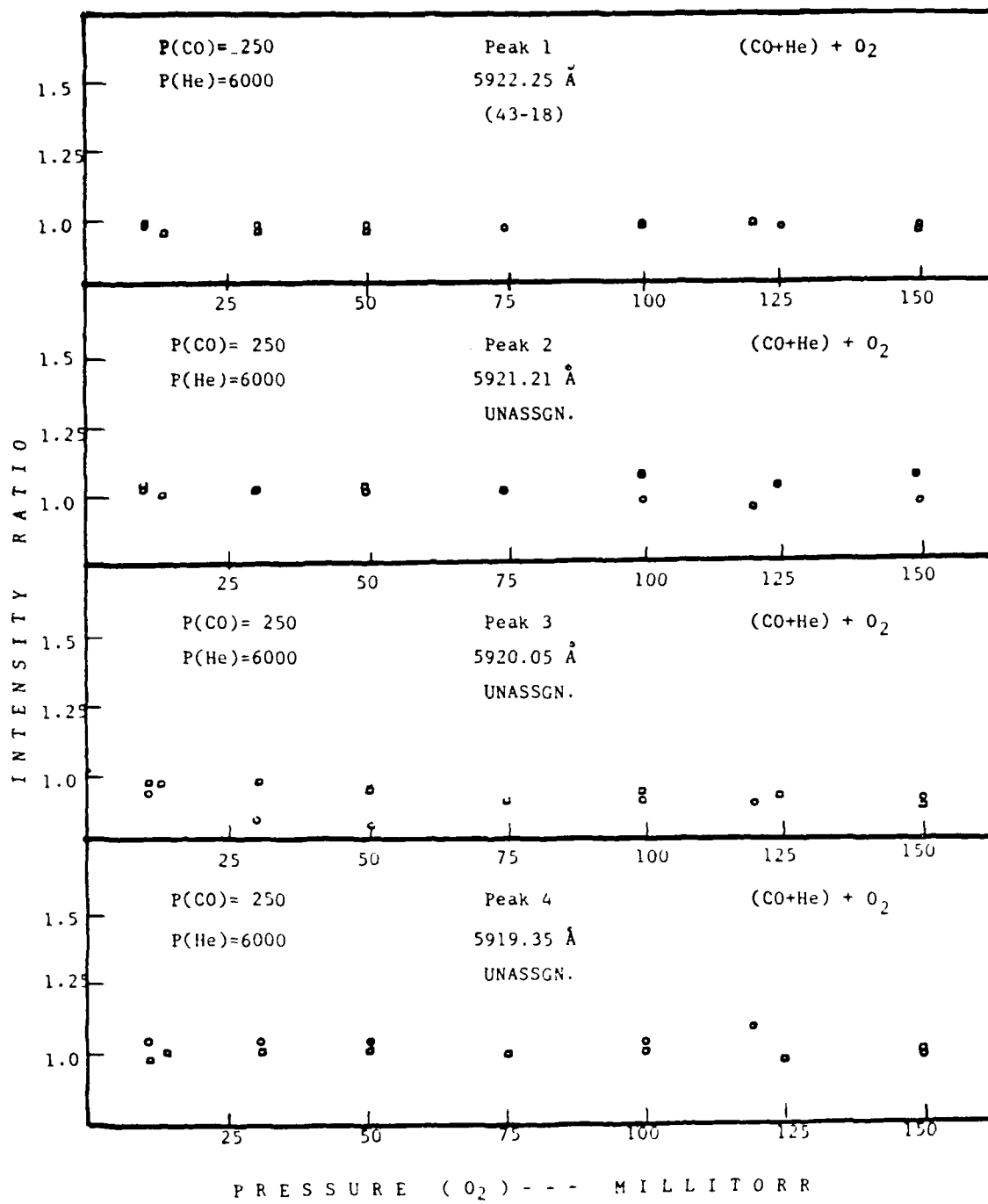
Previous studies involving CO-O₂ mixtures have reported anomalous effects on the efficiency that collisions have on vibrational relaxation. Some of it is accounted for by the chemical affinity between both collisional partners. Excitation of the gases creates numerous transient species as well as carbon complexes as final products from the chemical breakdown and reaction of CO. These reactions could influence the population of vibration levels of the electronic states which we observe in our spectra. The efficiency of V-V energy transfer is also affected by the rate of vibrational to translation energy (V-T) transfer where such a transfer is more dominant at the higher vibrational levels. There are numerous other competing mechanisms that could influence the intensity of those lines observed in our spectra.

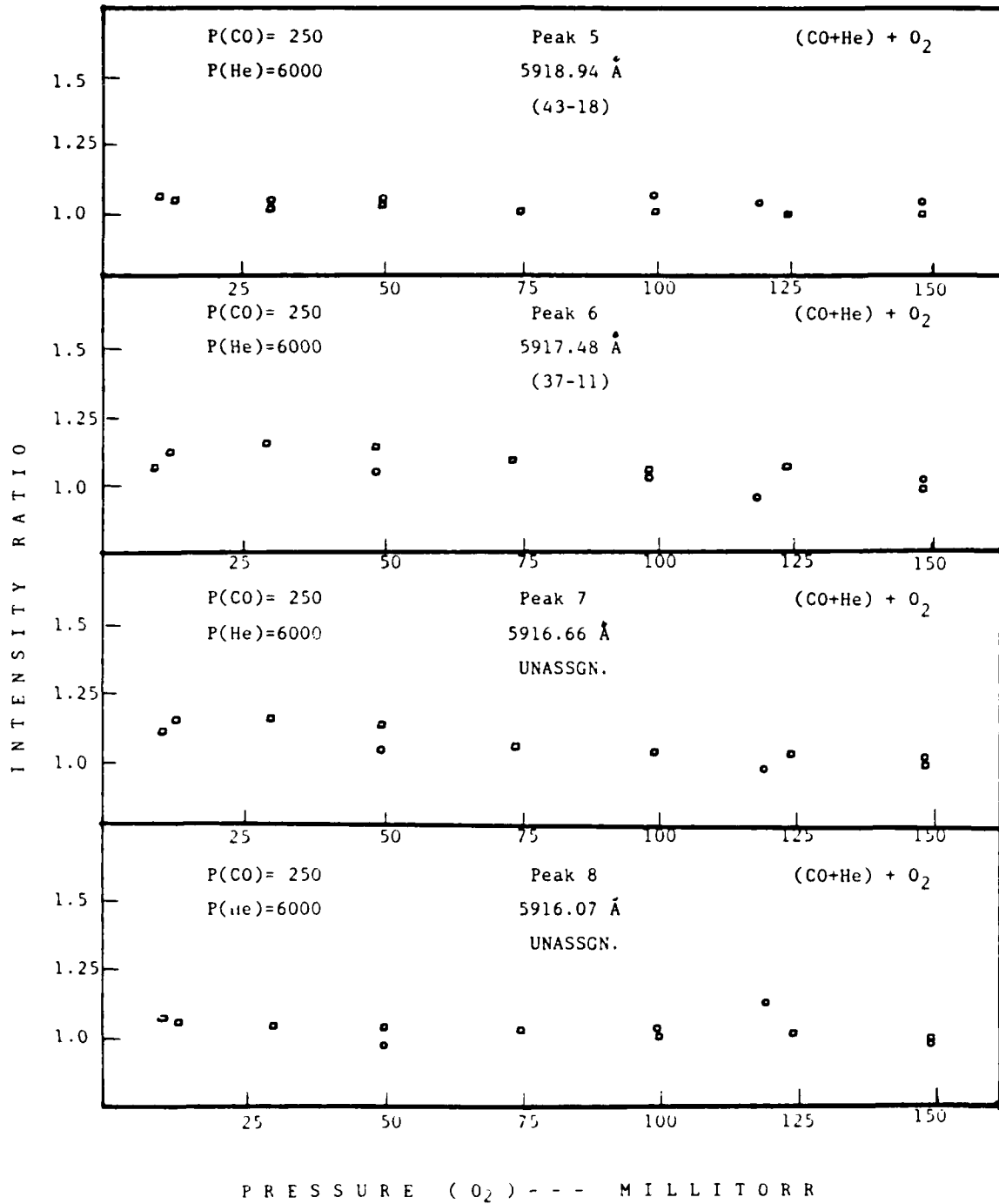
Mixtures of gases used in this study are similar to those used in the CO laser. Presently it is believed that oxygen does not play a role in energy transfer from itself to CO since the optimum amount of O₂ in the laser discharge is quite small. However, despite the difficulties in analyzing the spectra and the influence of other competing energy transfer mechanisms, oxygen does show an anomalous effect on the CO spectrum indicating the possibility of resonance vibrational energy transfer from CO to O₂.

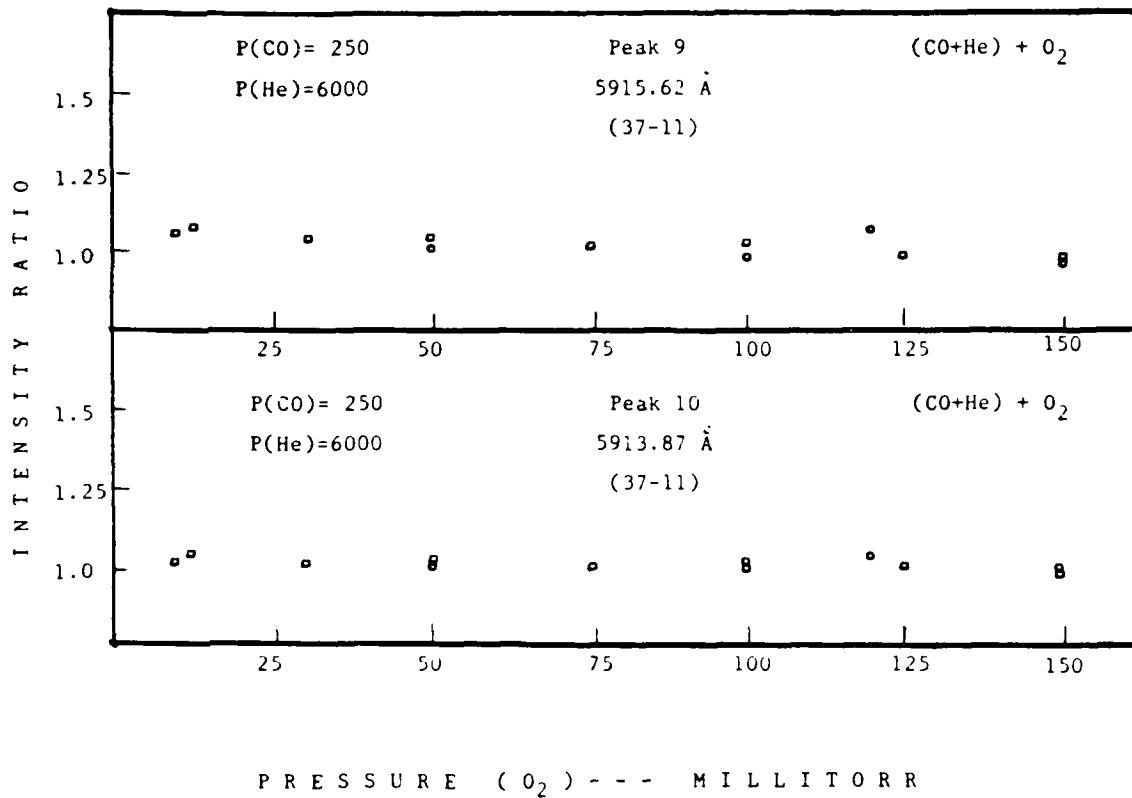
APPENDIX A

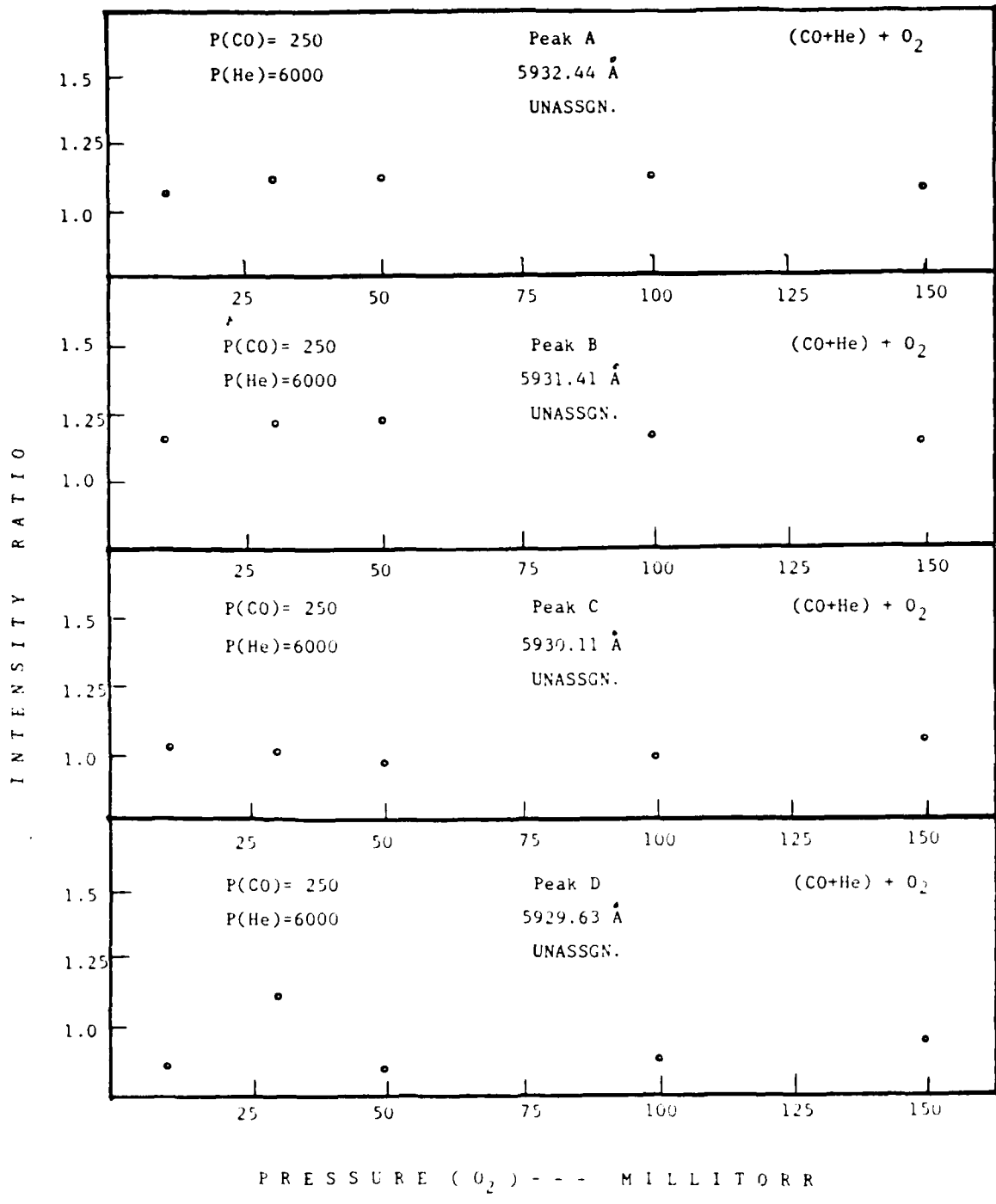
PLOTS OF INTENSITY RATIO vs. O₂ PRESSURE FOR REGION A (WITH HELIUM)

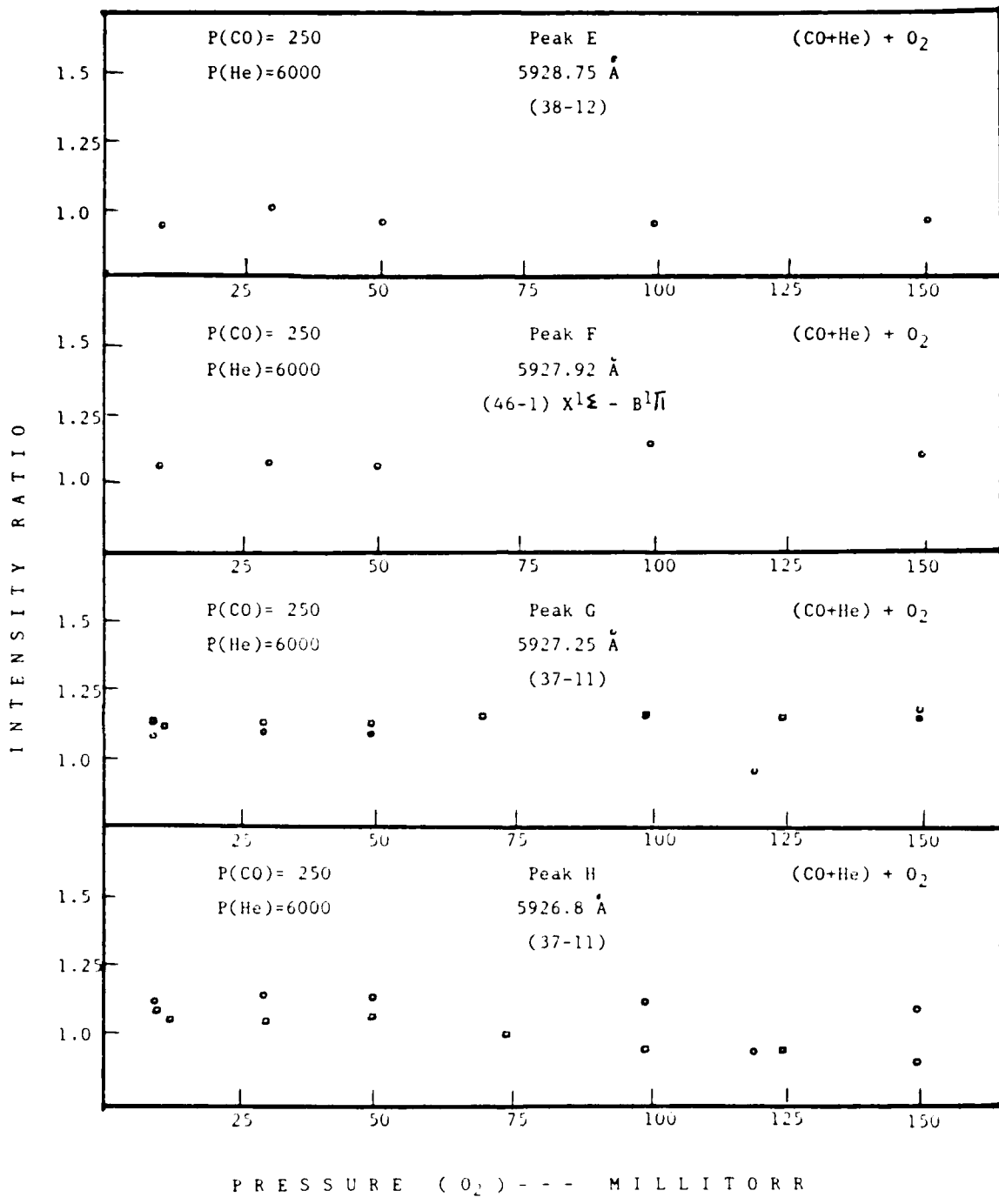
Plots of Intensity Ratio versus O₂ Pressure for selected peaks within Region A (5913 - 5923 Å) and for those in adjacent spectral regions are shown. Helium at 6 Torr and CO at 0.25 Torr vs. added partial pressures of O₂ are displayed. Peaks labeled with numbers are those within Region A and those with letters are outside of the region. Unless otherwise noted, assigned vibrational bands belong to the Fourth Positive System ($X^1\Sigma - A^1\pi$) of CO. Values for pressure are in units of Millitorr. Pages A-2 thru A-4 show data of peaks within Region A and Pages A-5 → A-8 are for those outside the region. See Fig. 4.5 for locations of peaks as they are identified on the CO spectrum.

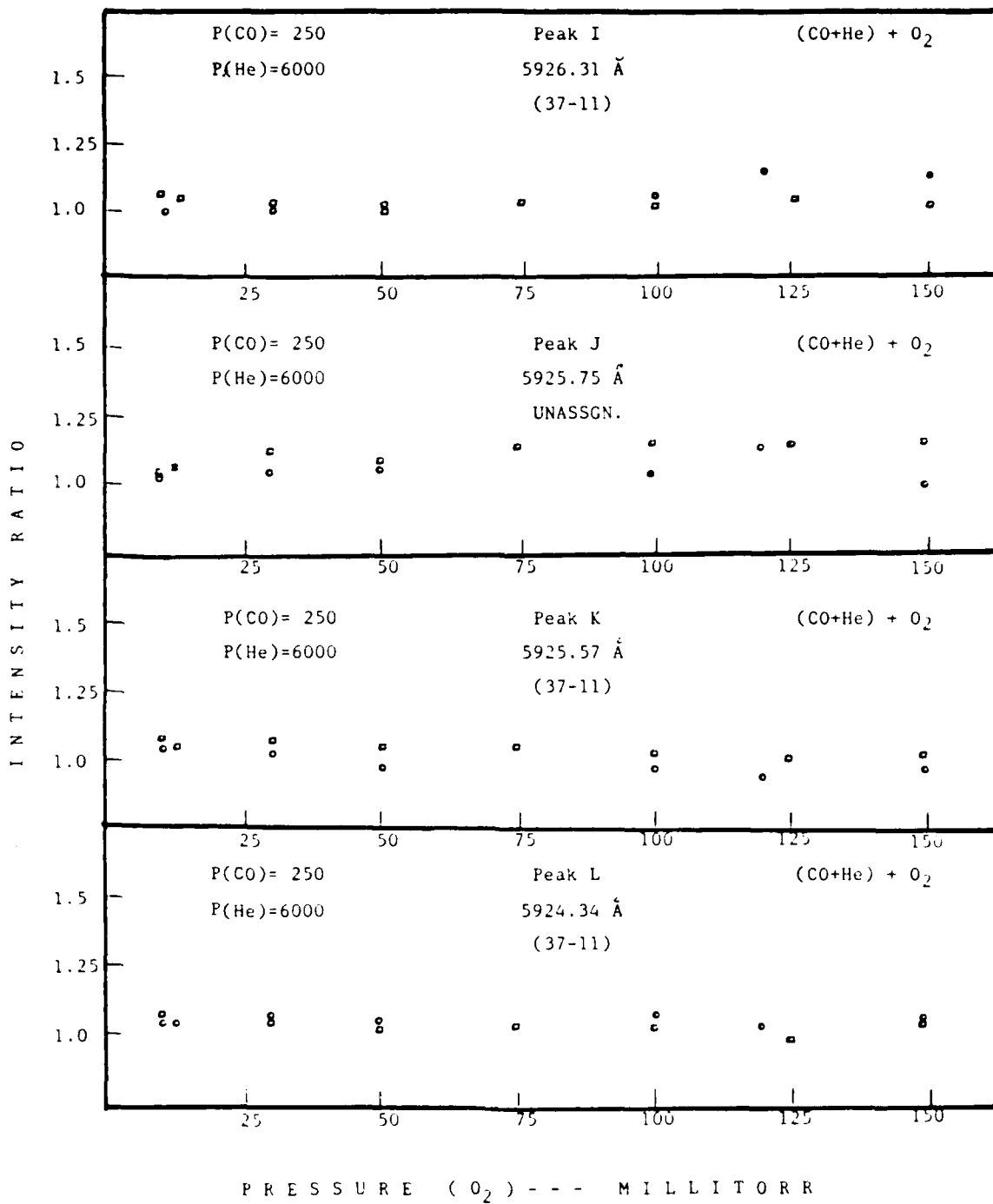


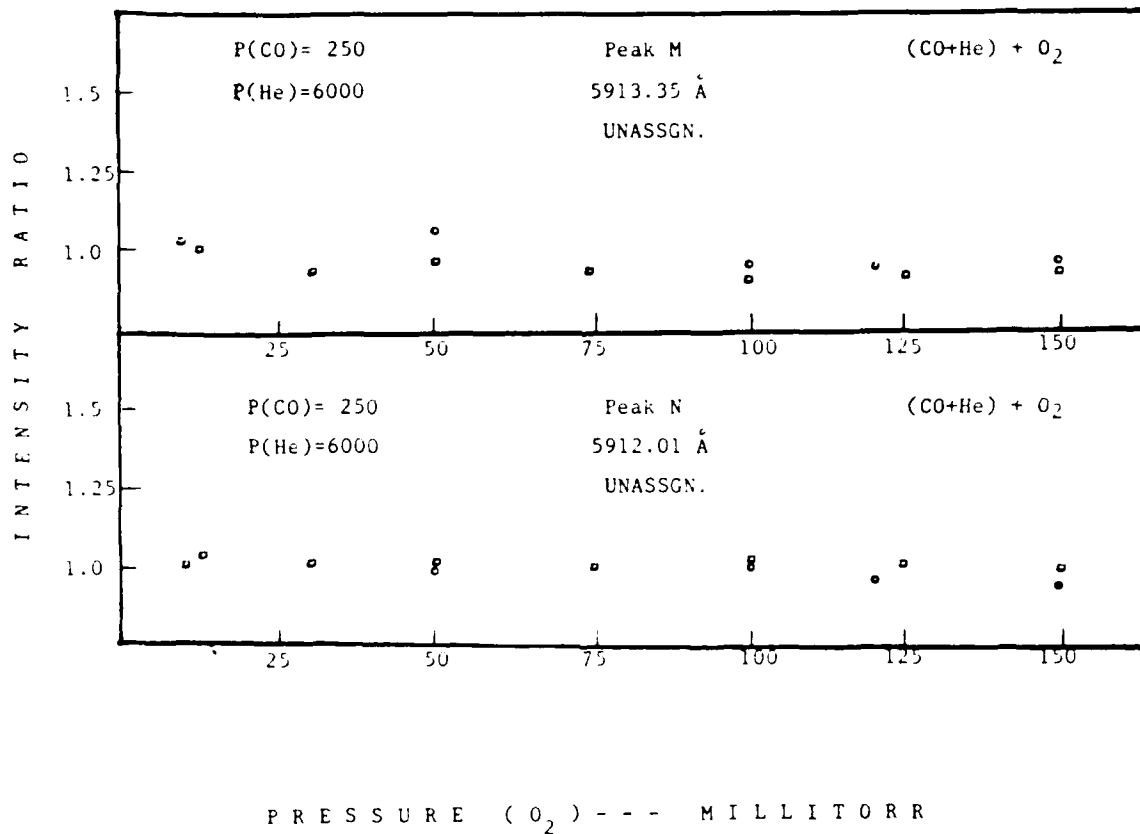








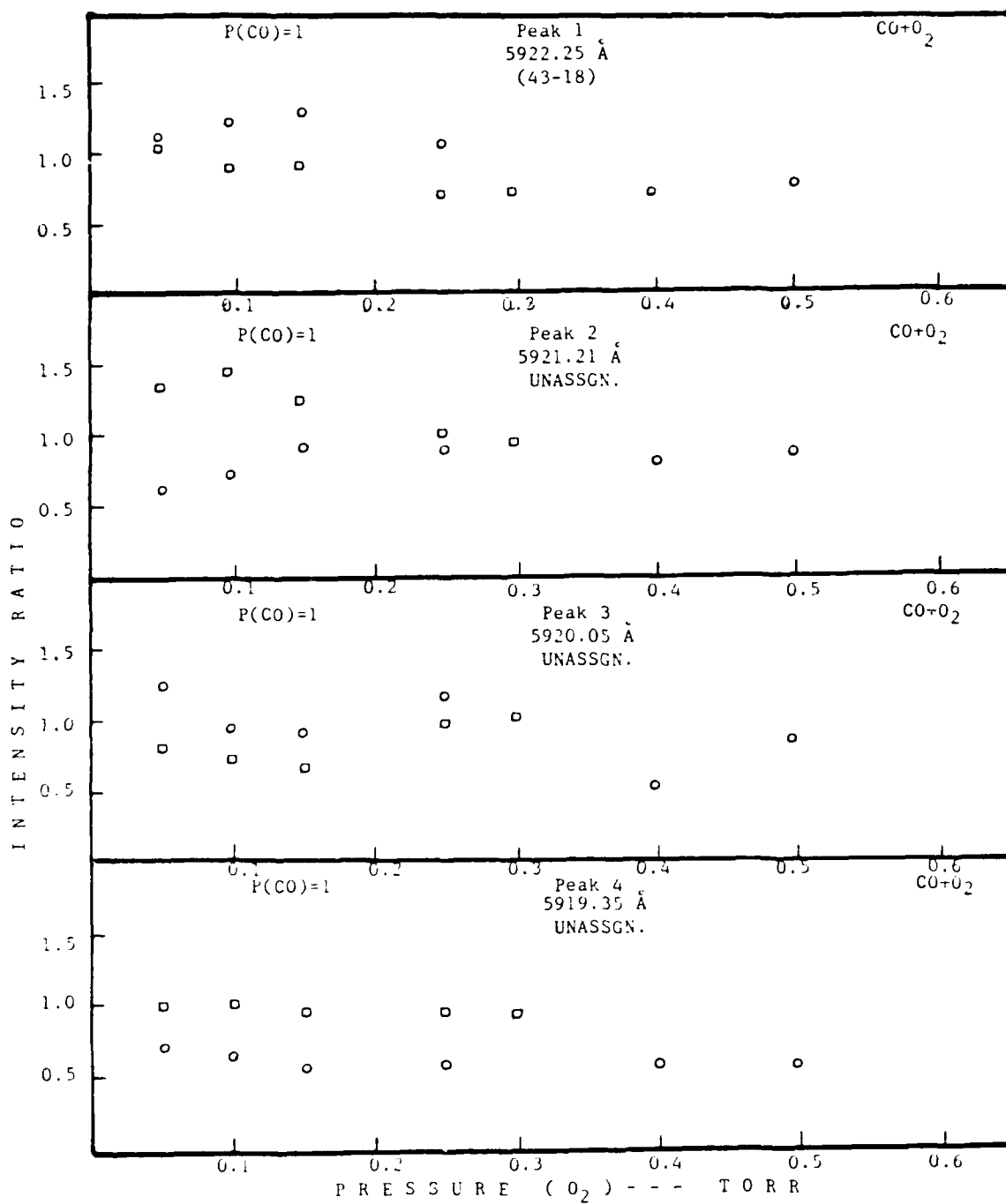


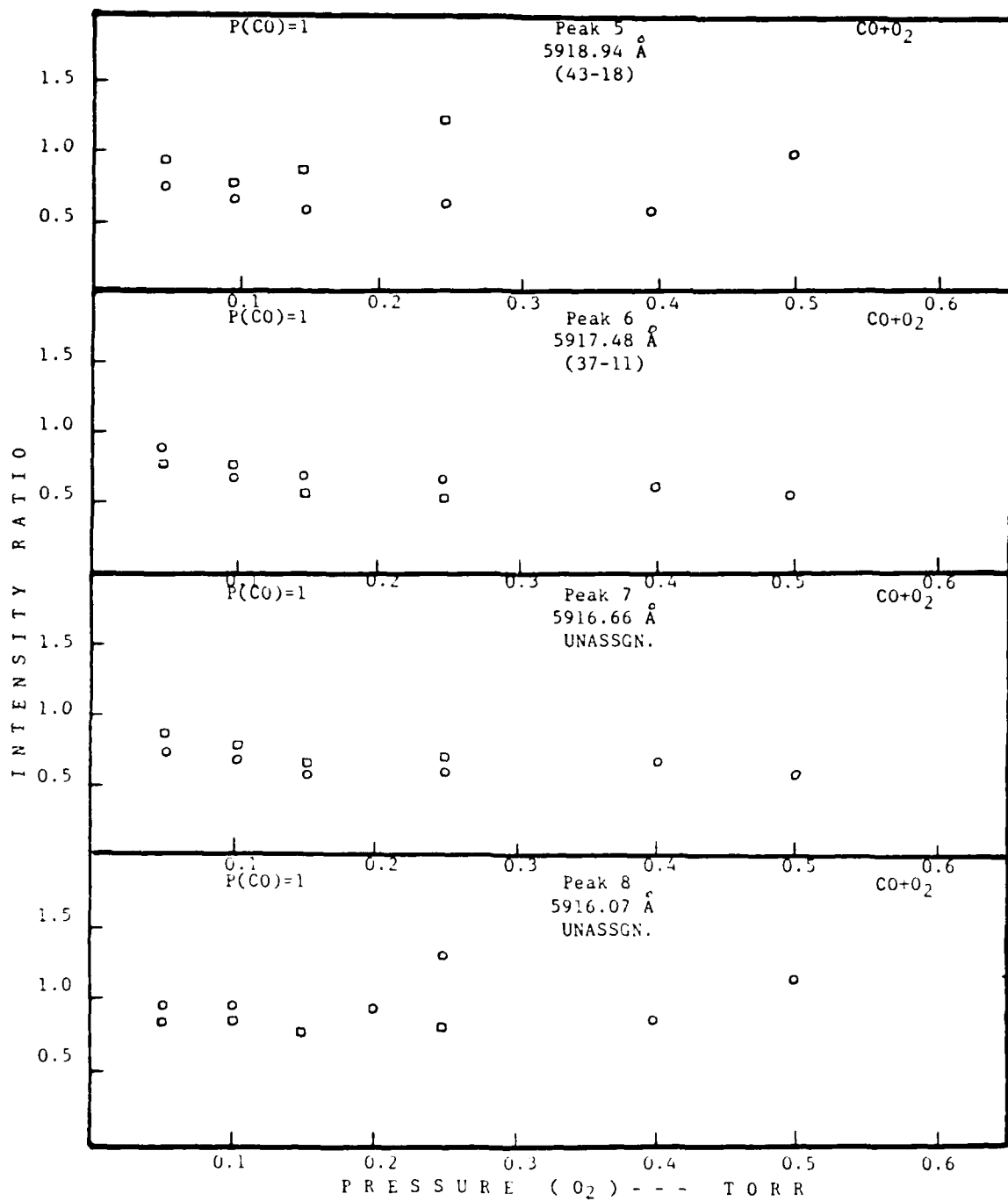


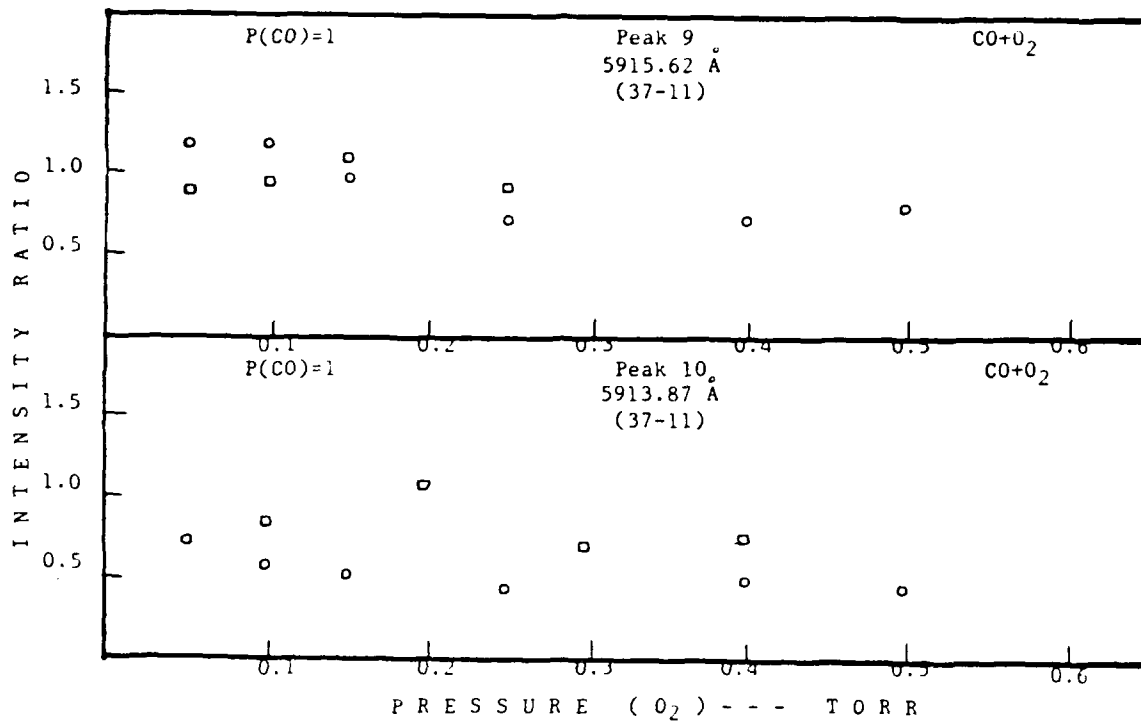
APPENDIX B

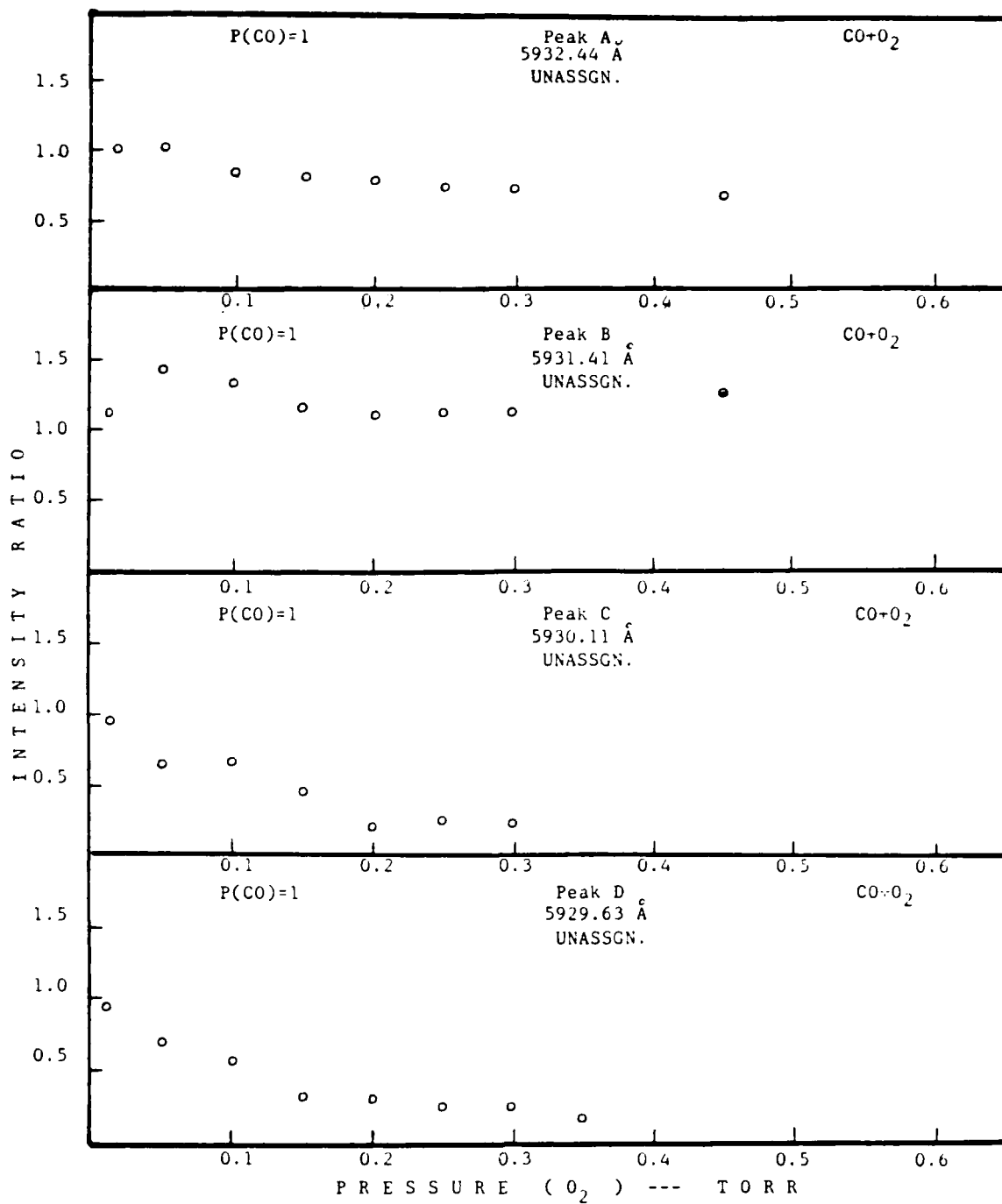
PLOTS OF INTENSITY RATIO vs. O₂ PRESSURE FOR REGION A (WITHOUT HELIUM)

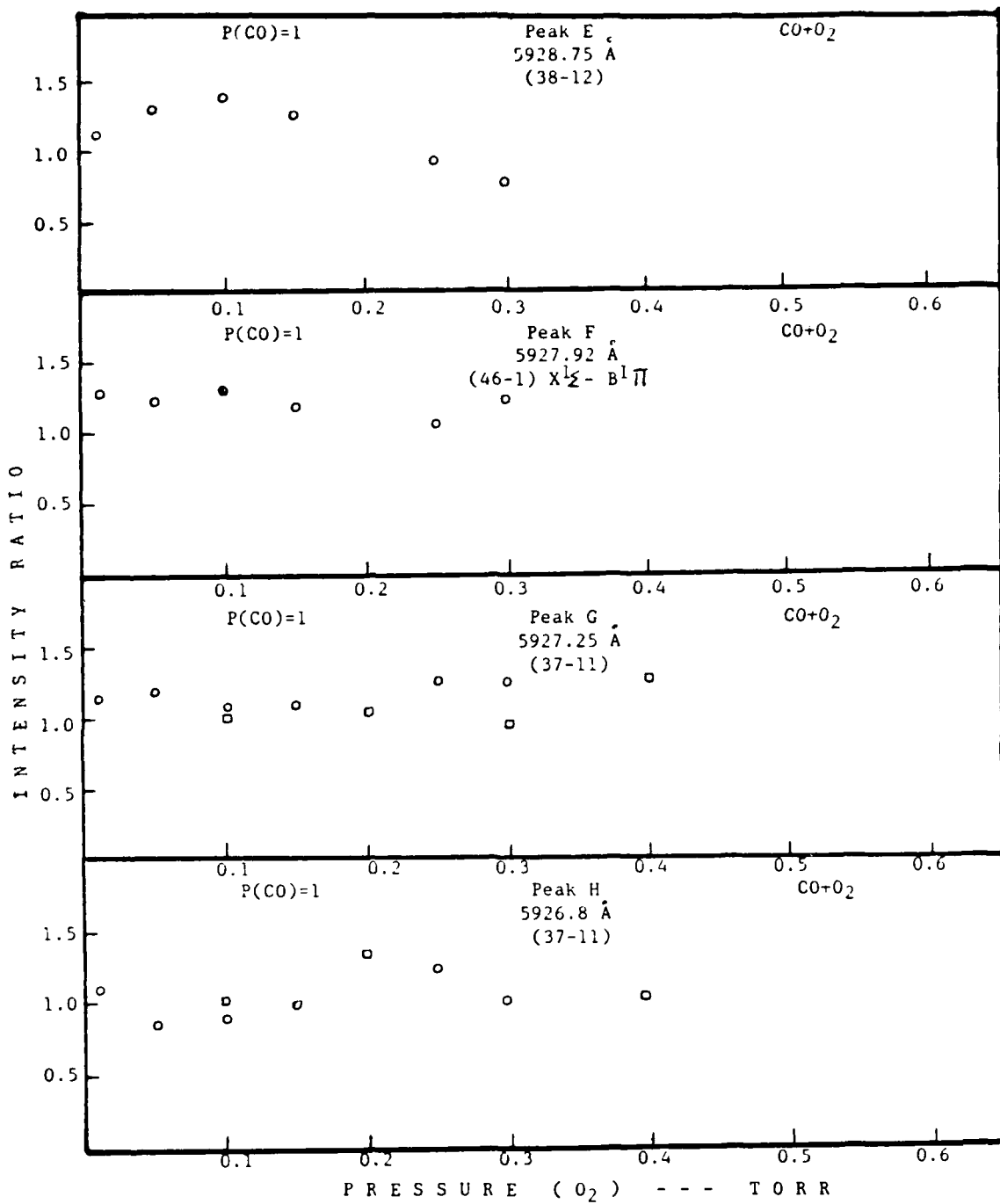
Plots of Intensity Ratio versus O₂ Pressure for the same peaks in Region A (5913 - 5923 Å) as shown in Appendix A are displayed but without helium included in the mixture. Values for pressure are in units of Torr. Numbered peaks are those in Region A and lettered peaks are those located in adjacent regions outside of Region A. See Fig. 4.5 for locations of peaks as they are identified on the CO spectrum.

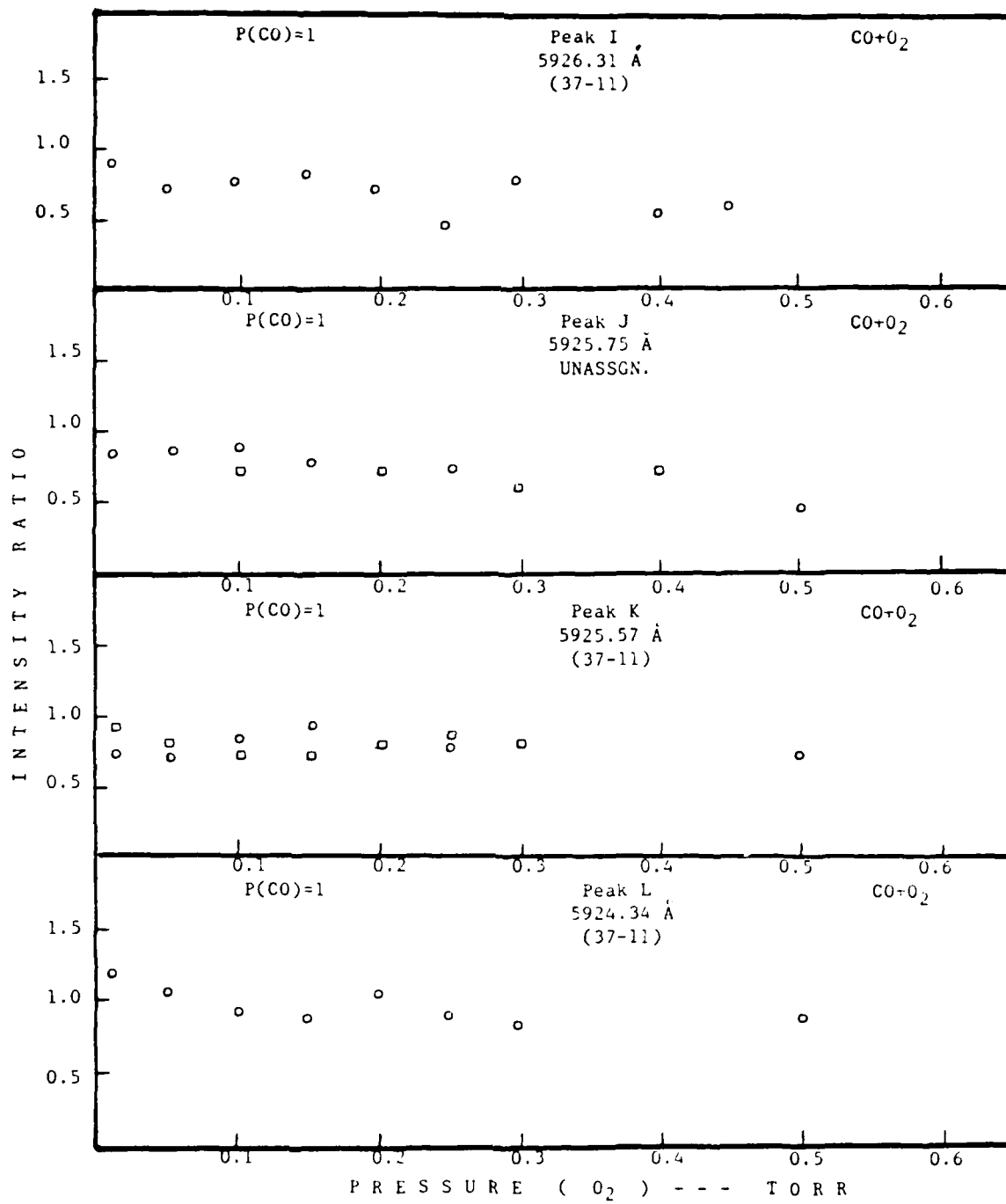


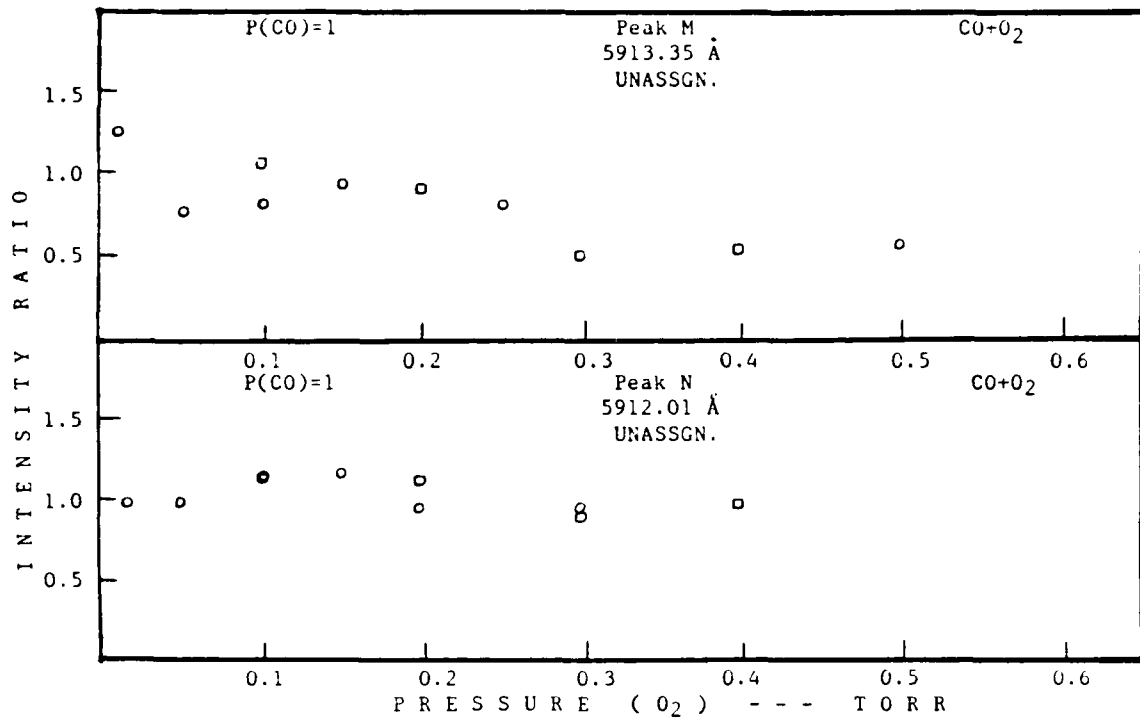








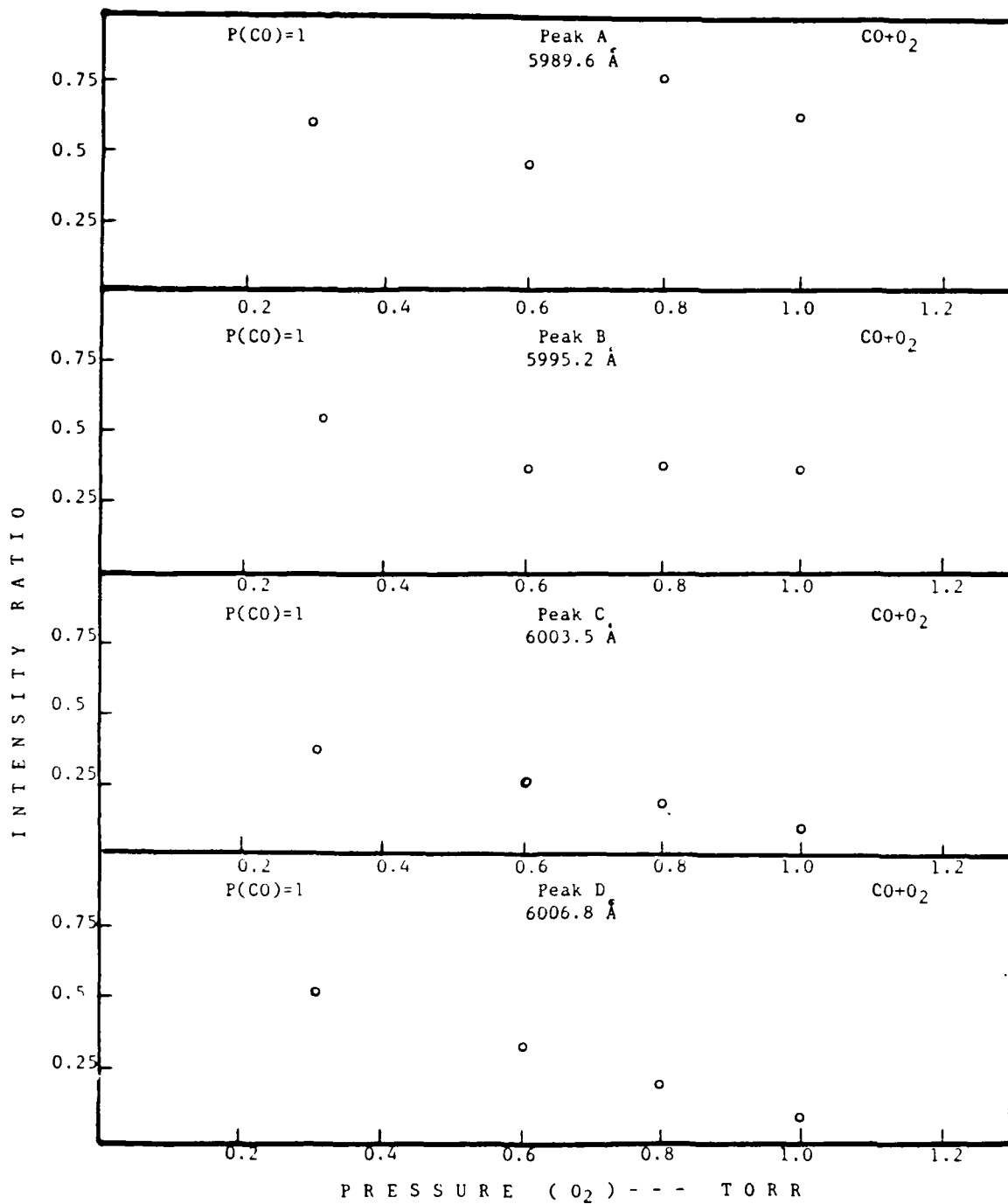


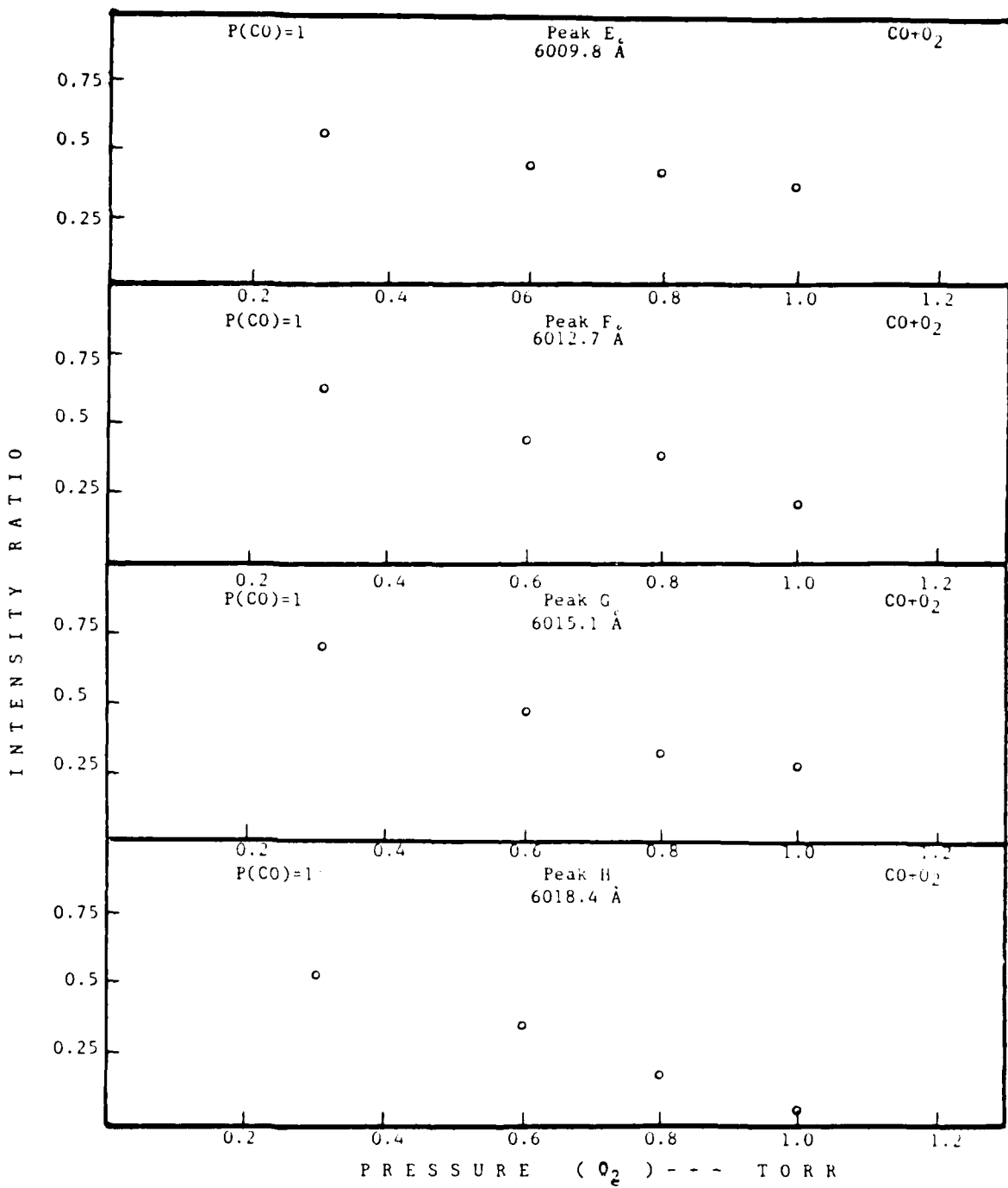


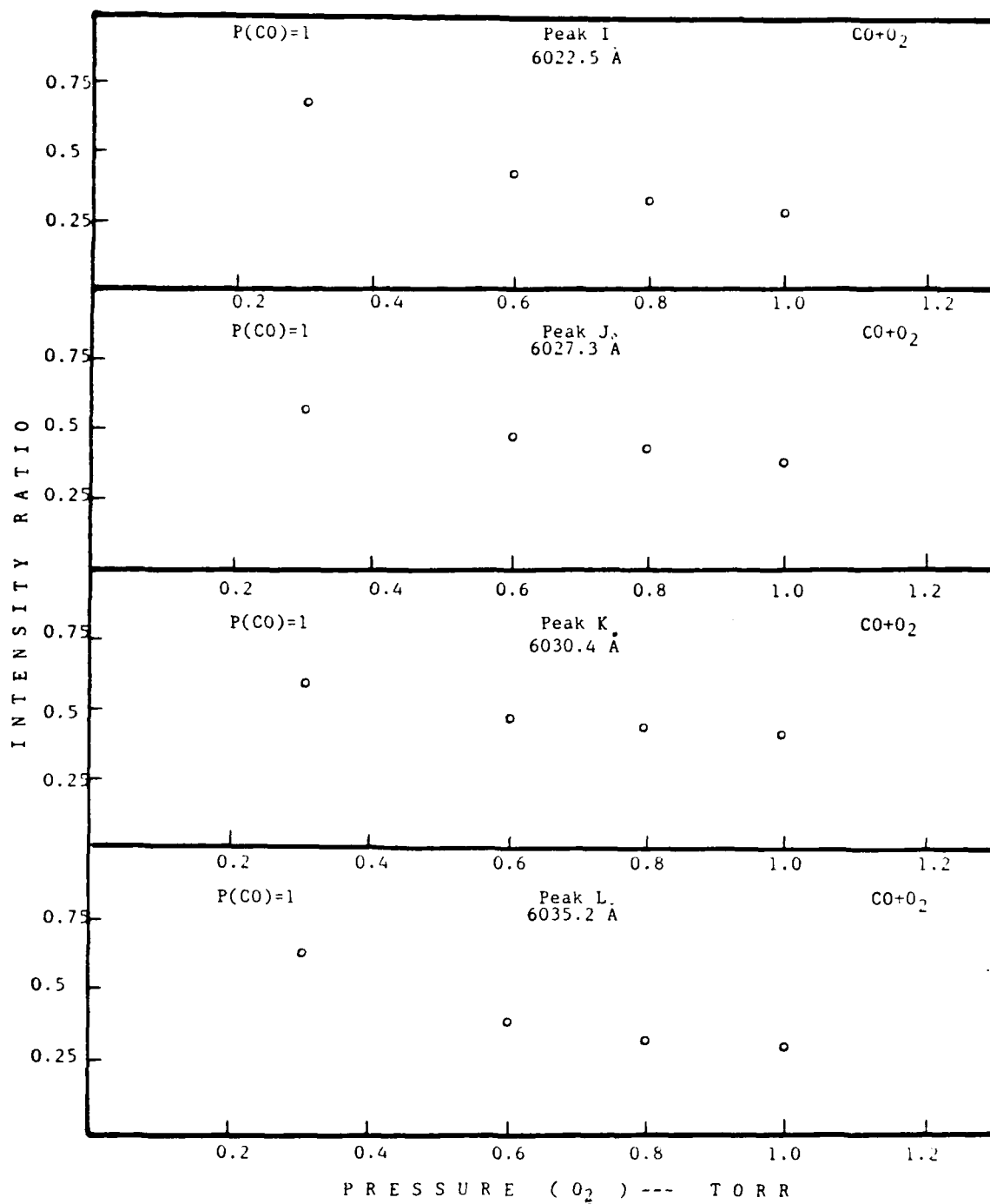
APPENDIX C

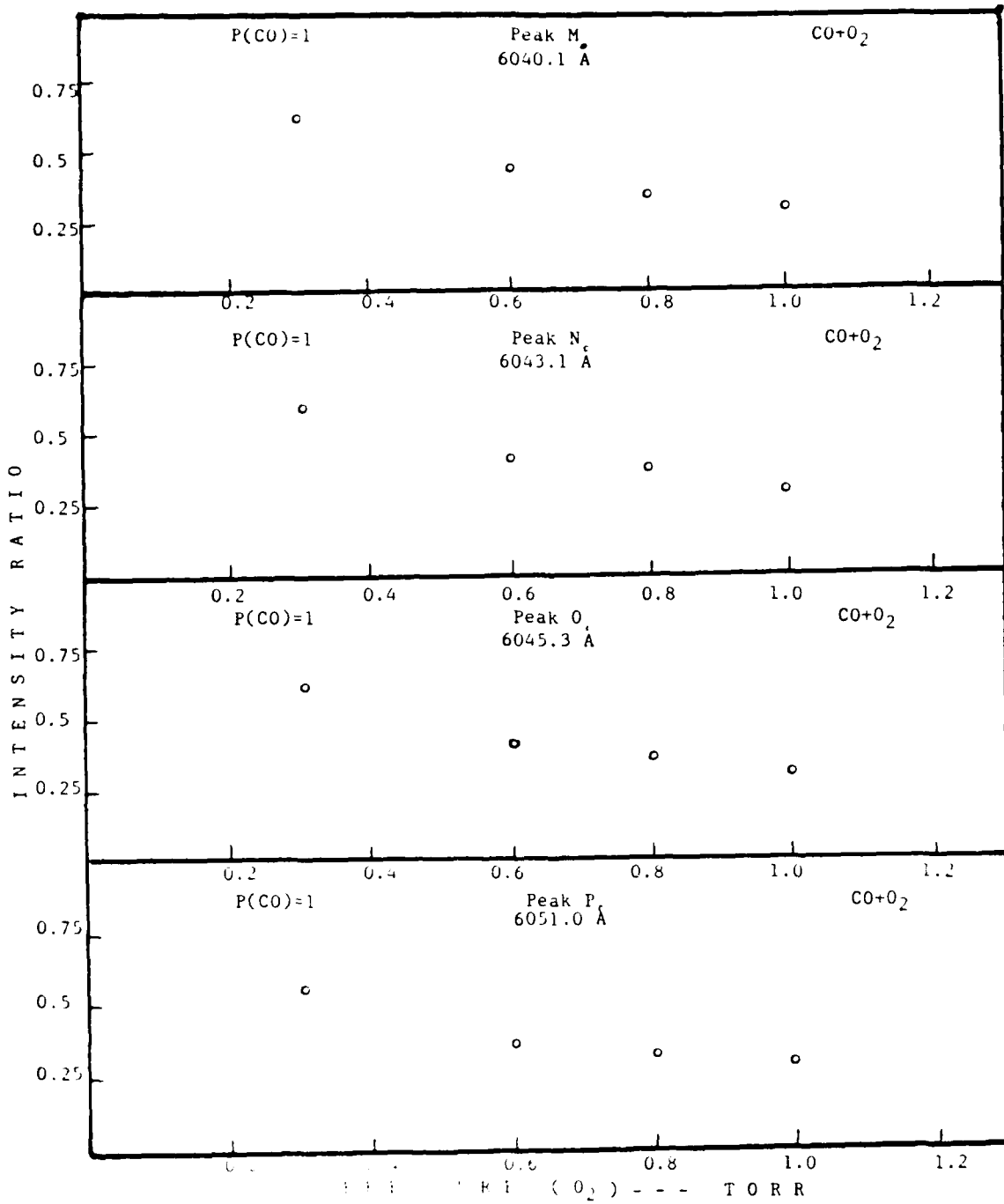
PLOTS OF INTENSITY RATIO vs. O₂ PRESSURE FOR SPECTRAL REGION 5990 - 6075 Å (REGION E)

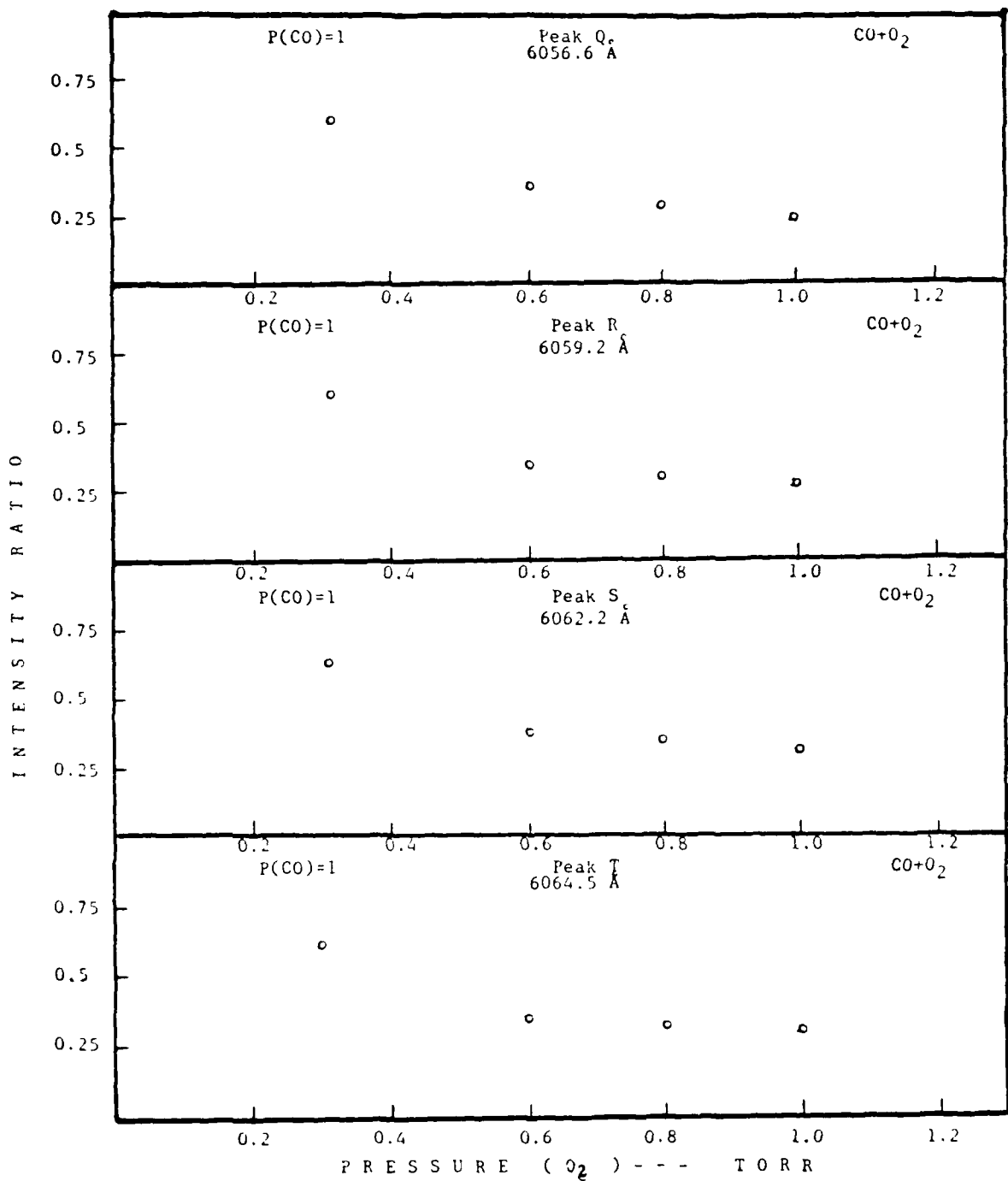
Plots of Intensity Ratio versus O₂ Pressure for selected peaks within Region E (6000 - 6030 Å) and adjacent spectral regions are shown. This region (5990 - 6075 Å) for pure CO shows relative high intensities for lines throughout. Peaks in Region E have not been designated differently since the trend of decreasing intensity over increased oxygen is the same for the entire region. Helium was not included in the mixture. See Fig. 4.7a for locations of peaks as they are identified on the CO spectrum. Values for pressure are in units of Torr.

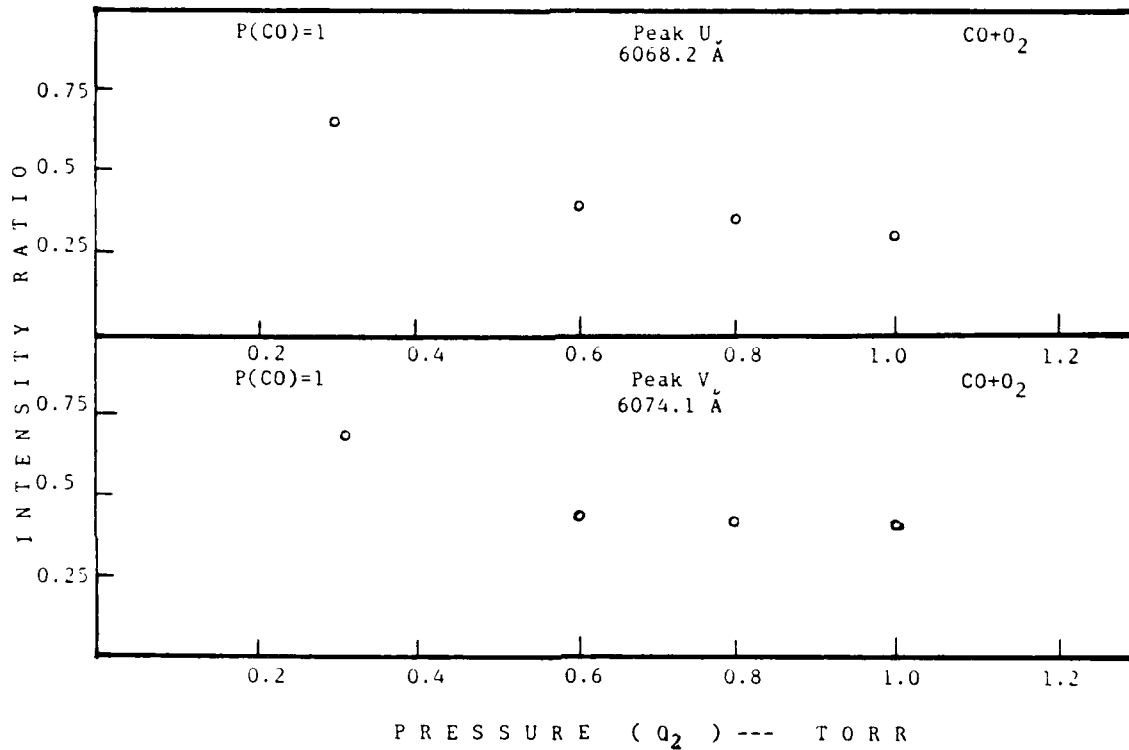












5